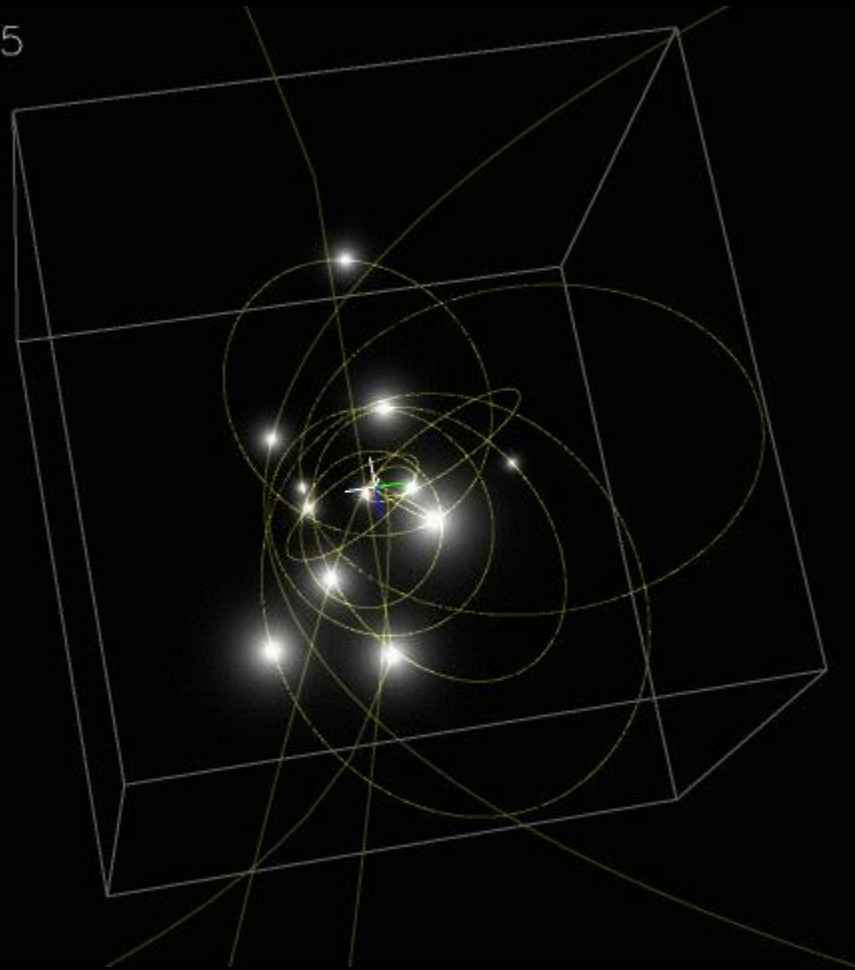


# *ESTRUCTURA GALÁCTICA Y DINÁMICA ESTELAR*

*El Centro Galáctico*

# *El Centro Galáctico*

Year: 1995.5



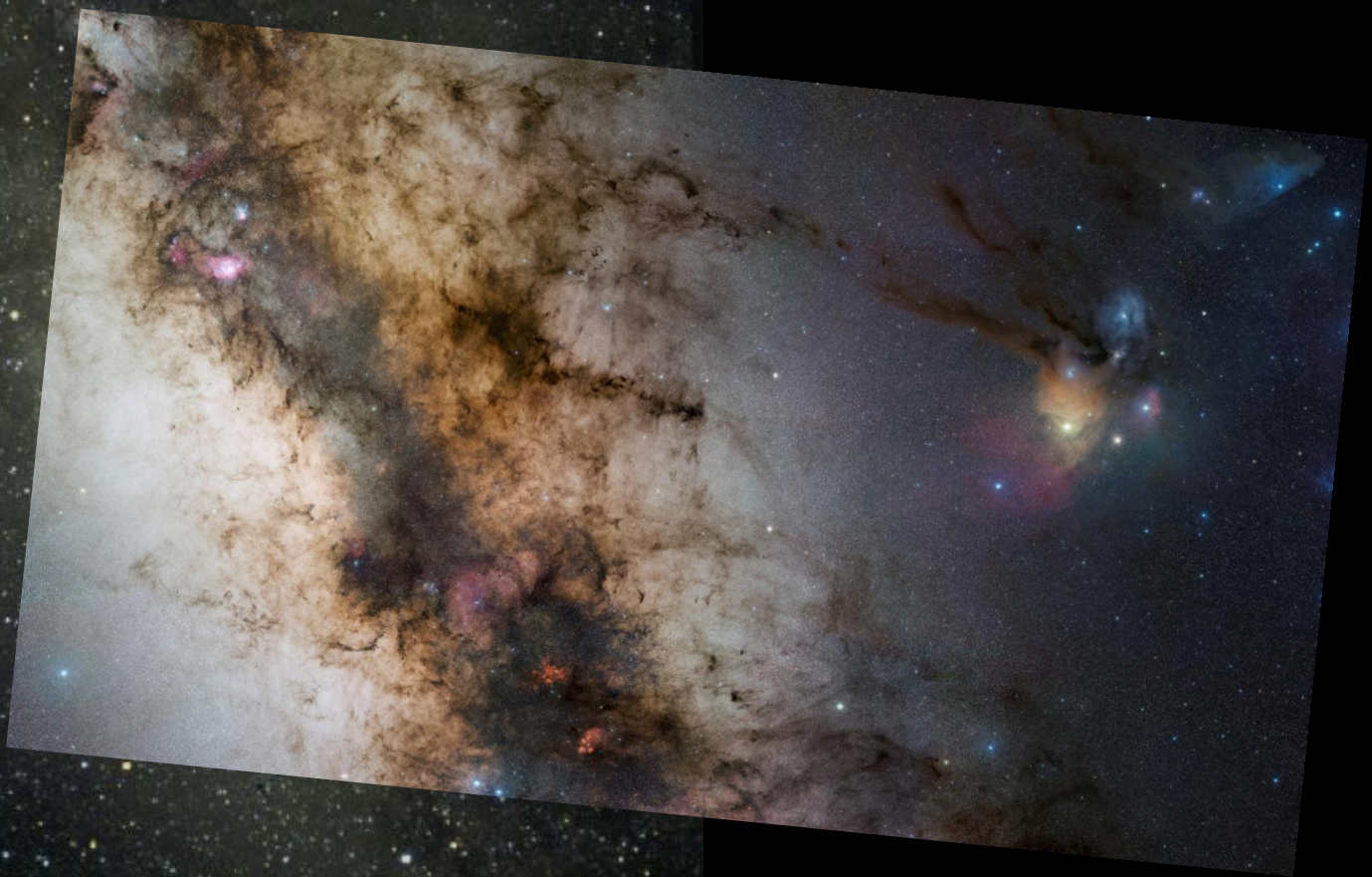
# Hacia el Centro de la Vía-Láctea

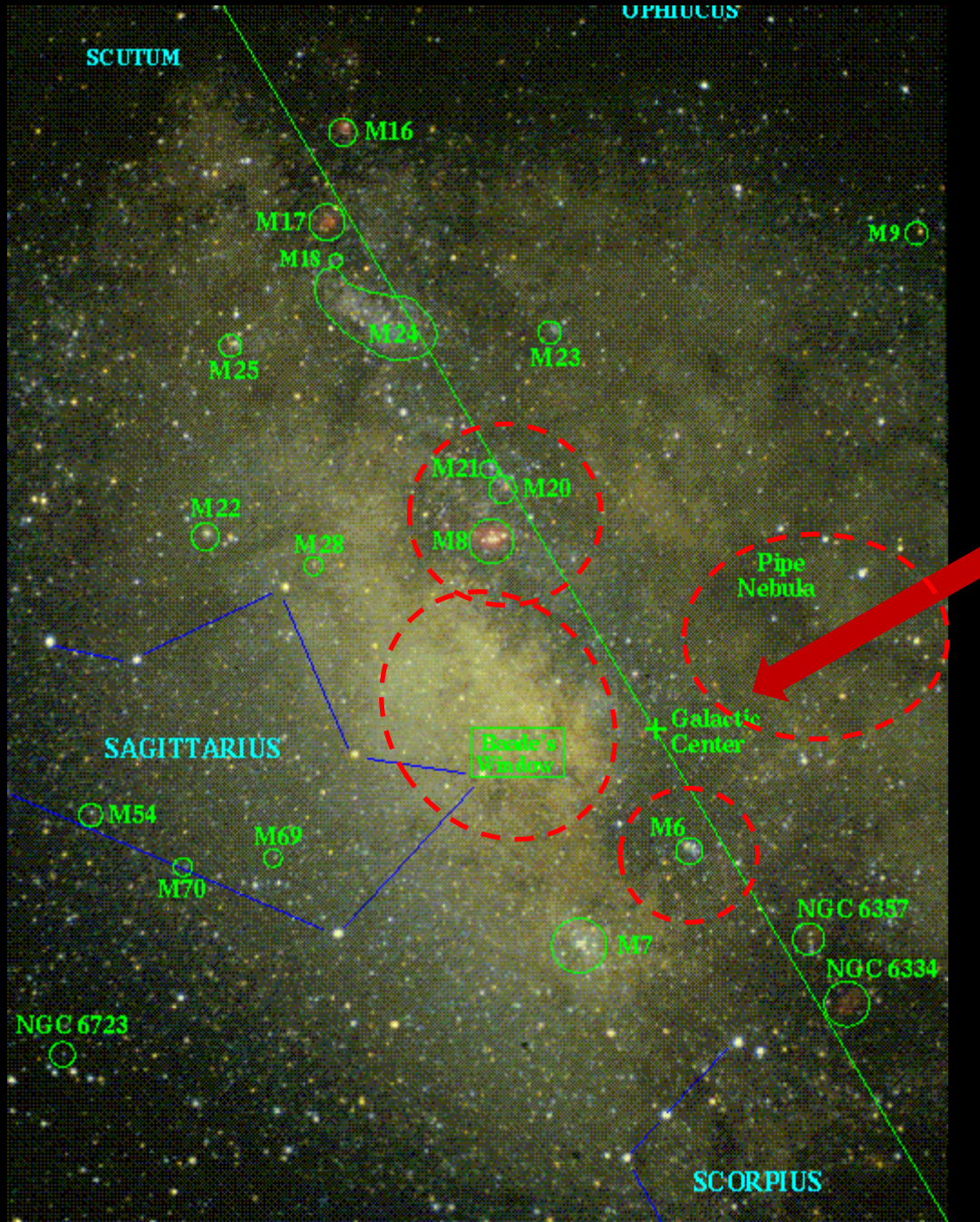


$27^\circ \times 40^\circ$  ( $\sim 5.6$  kpc)

Óptico

CTIO (camera Canon)







NGC 6528  
(cúmulo globular, 7.9 kpc)

La Ventana de Baade

M20

M6 (cúmulo abierto  
“la Mariposa”, 0.5 kpc)

M20 (nebulosa Trífida, 1.6 kpc)

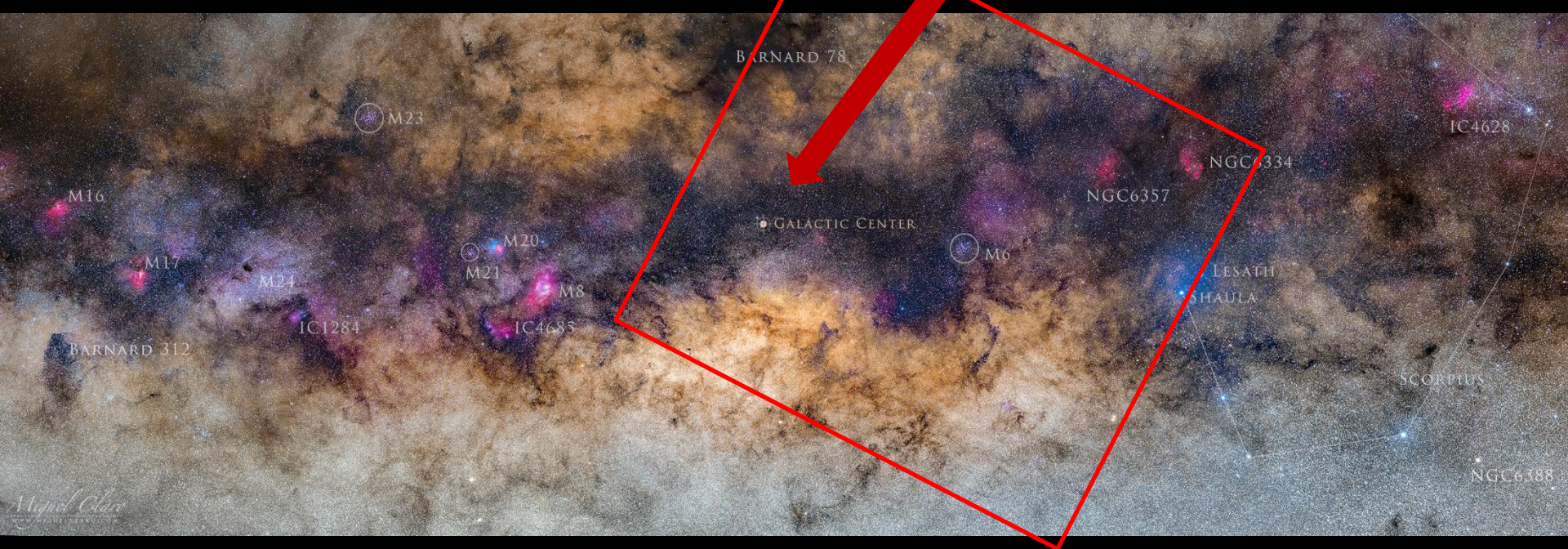


CTIO (camera Canon)

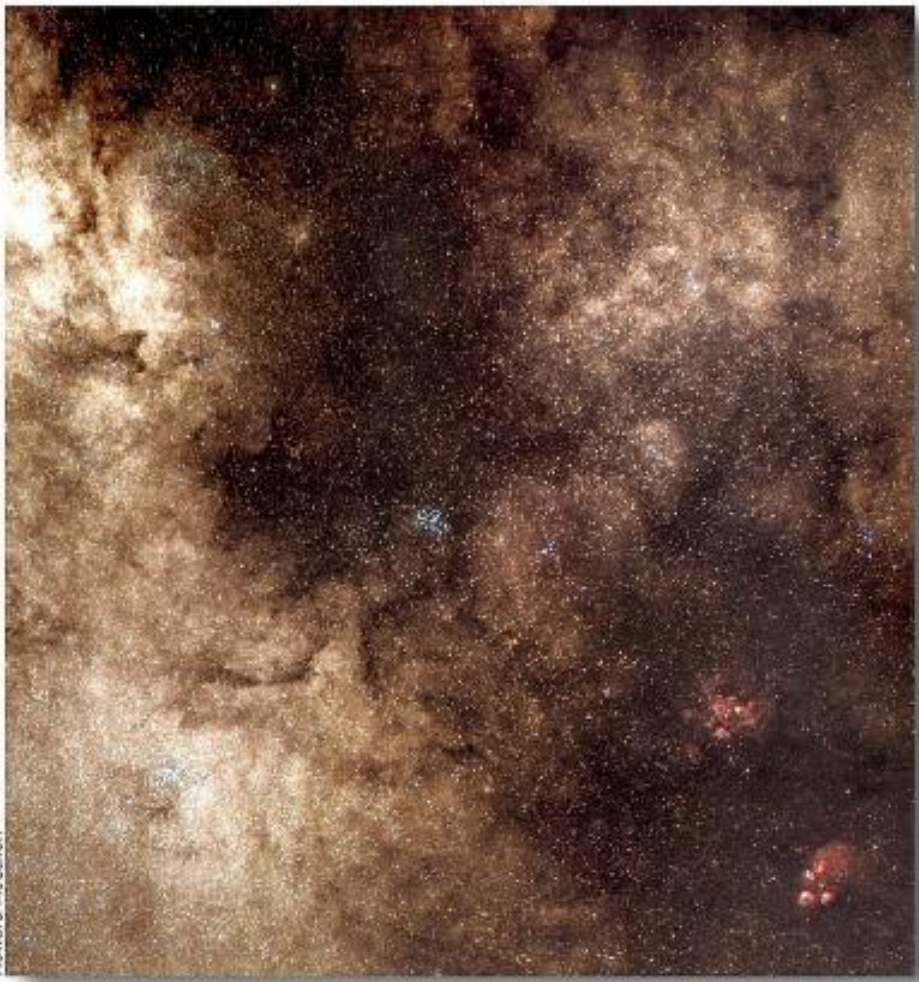
Centro  
Galáctico

$\alpha = 17^{\text{h}} 45.6^{\text{m}}$

$\delta = -28^{\circ} 56.2'$



# The Galactic Center



Howard McCallion  
Visible Light



Near Infrared/2MASS



Disco central  
de HI  
(de algunos  
cientos de pc  
hasta  $\sim$ 1-2 kpc,  
 $\sim 3 \times 10^7 M_{\odot}$   
de gas)



$8^{\circ} \times 10^{\circ}$  ( $\sim$ 1.4 kpc)

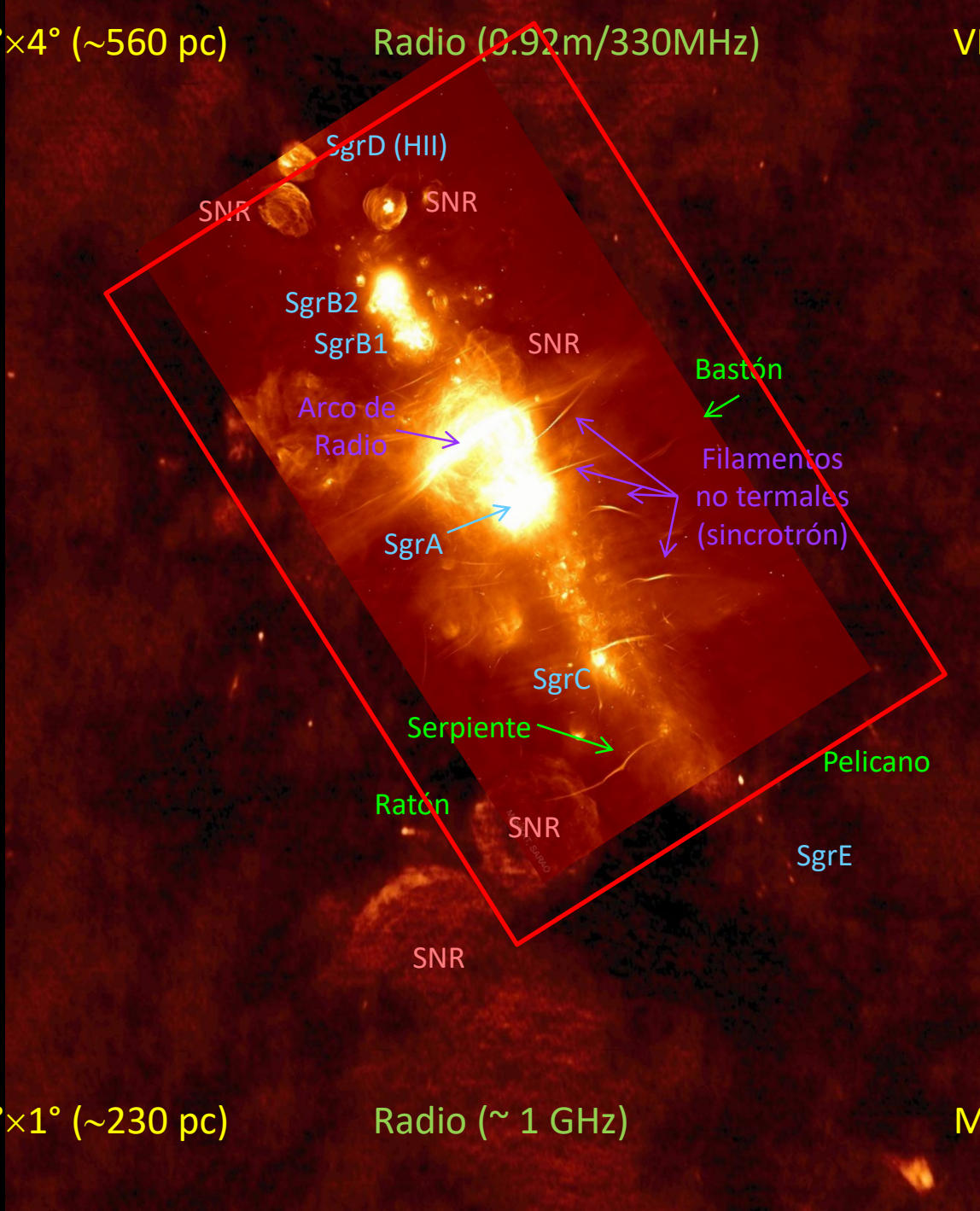
IR cercano (1.2-2.2  $\mu$ m)

2MASS

$4^\circ \times 4^\circ$  ( $\sim 560$  pc)

Radio (0.92m/330MHz)

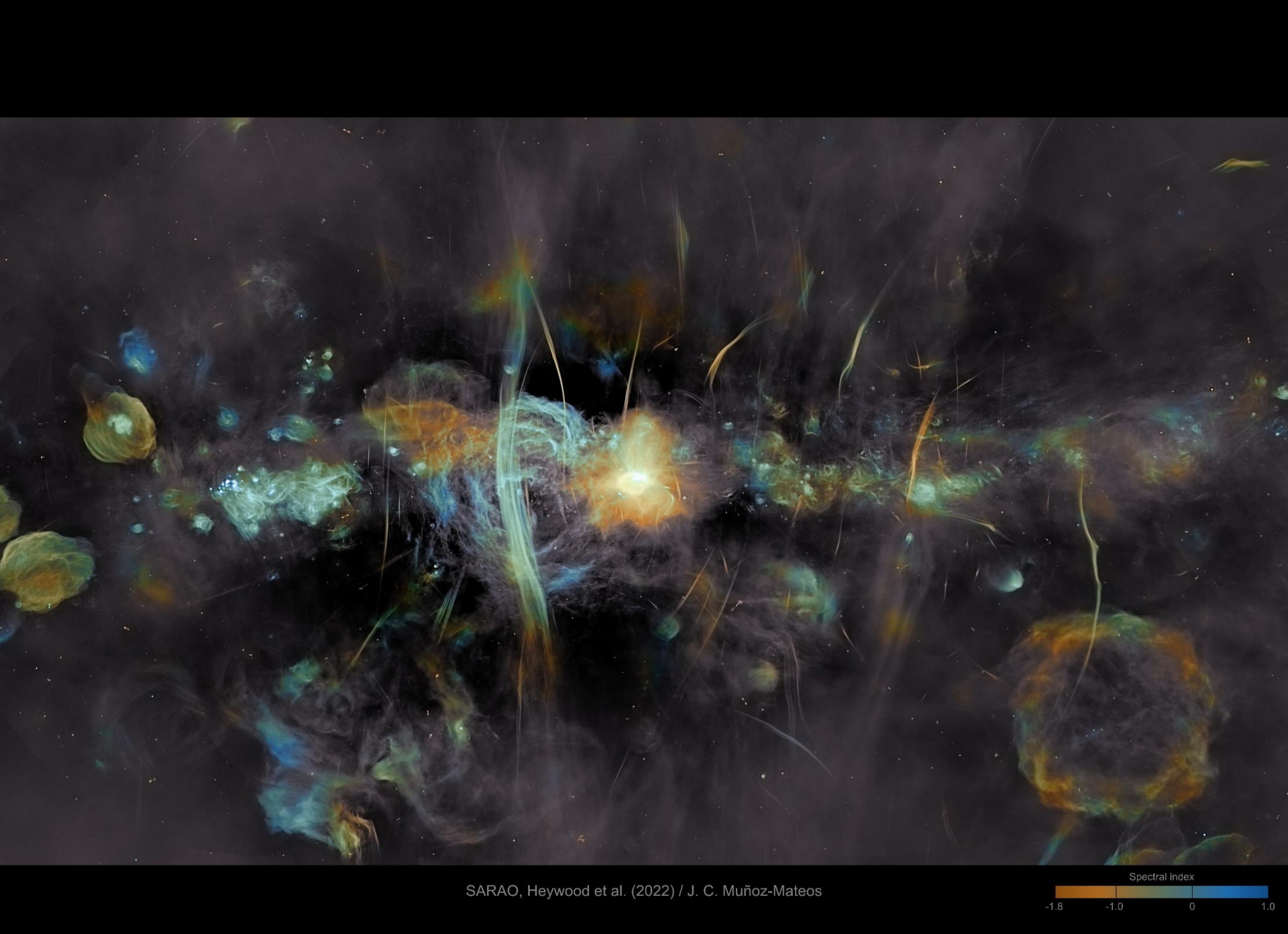
VLA

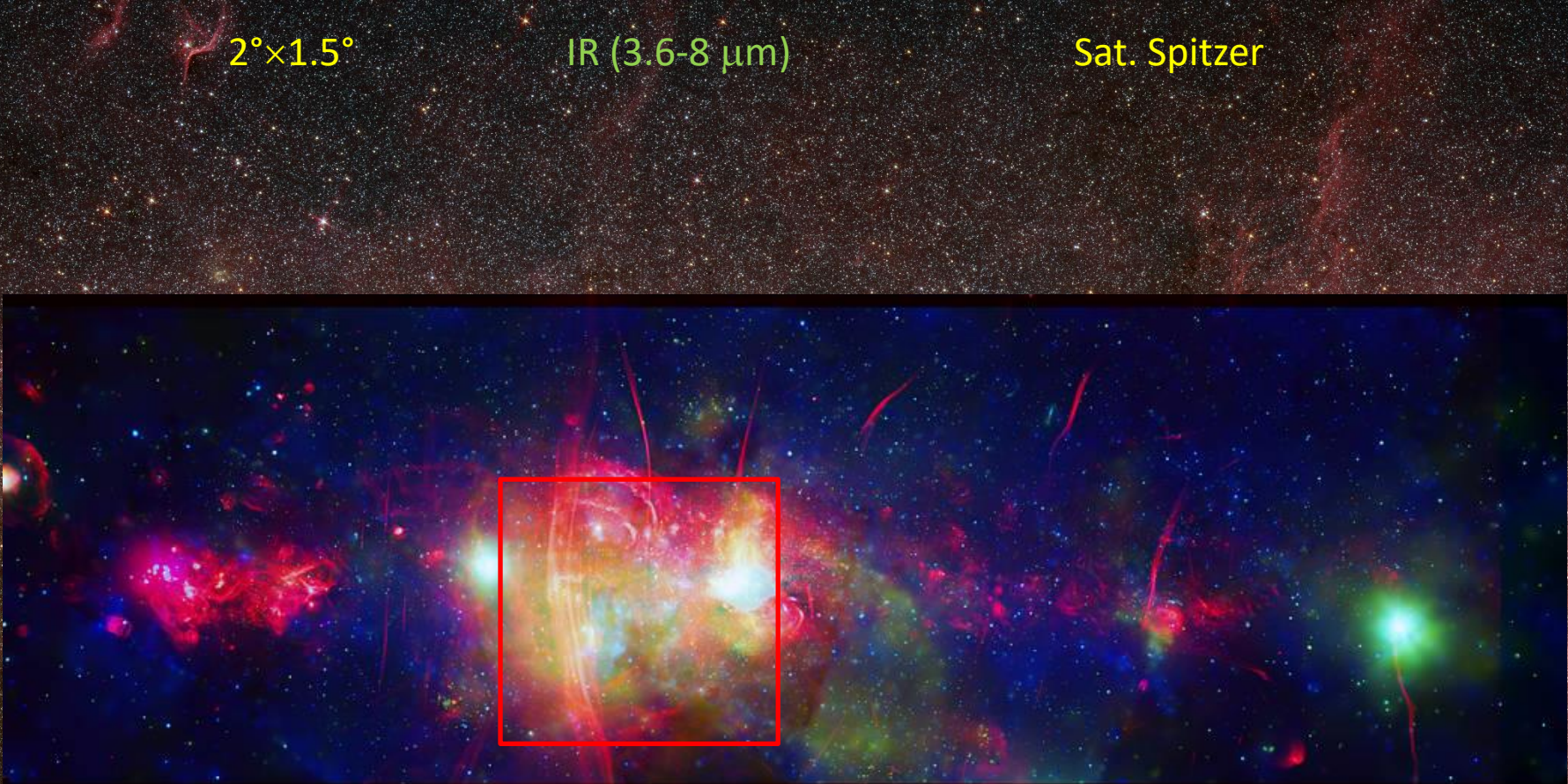


$2^\circ \times 1^\circ$  ( $\sim 230$  pc)

Radio ( $\sim 1$  GHz)

MeerKAT array



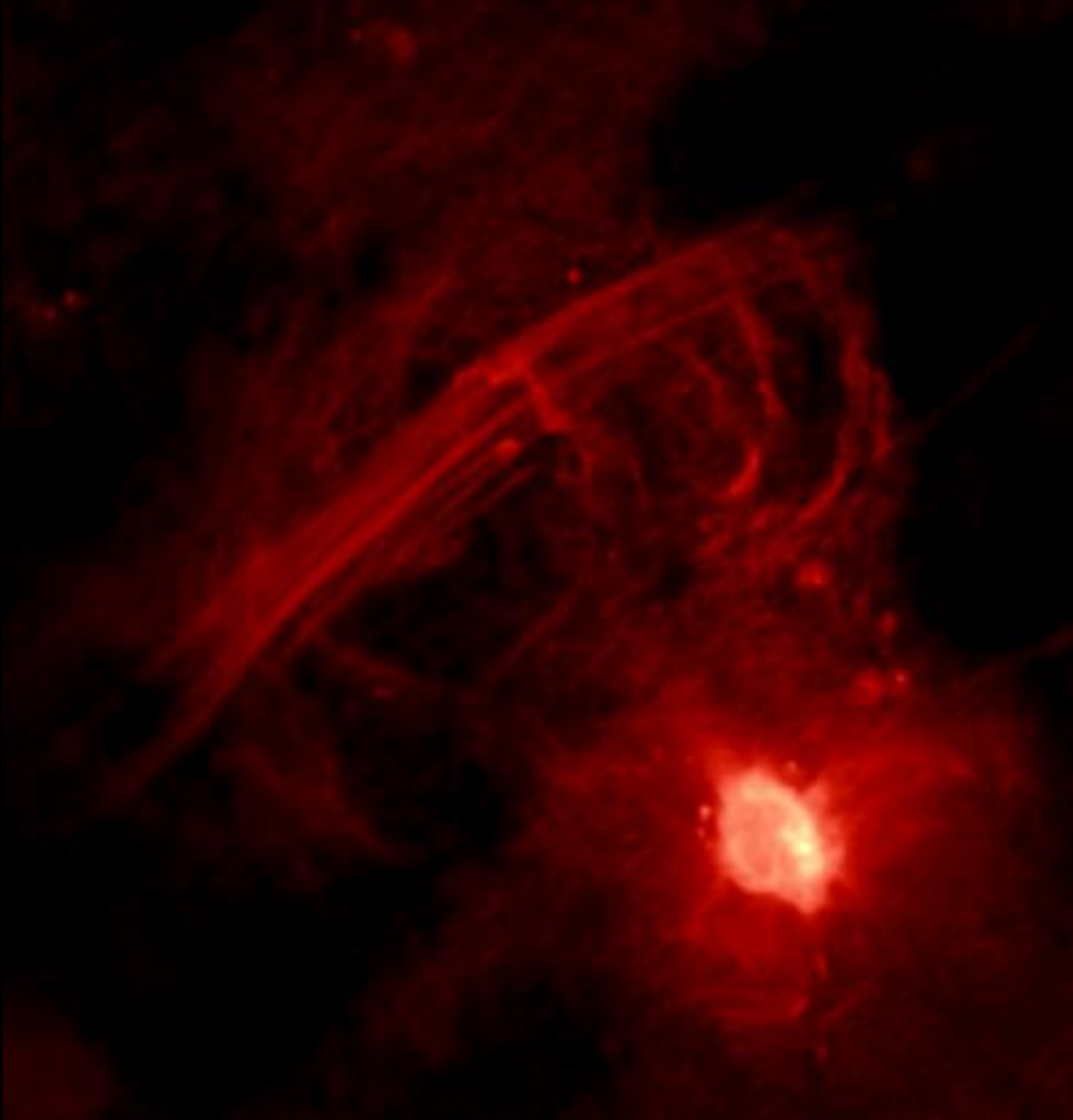


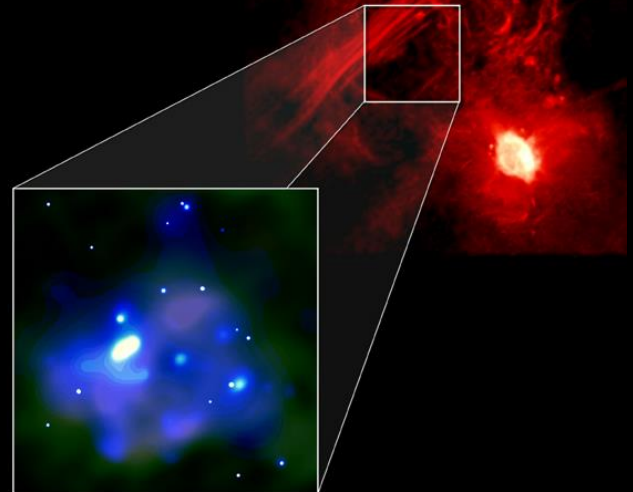
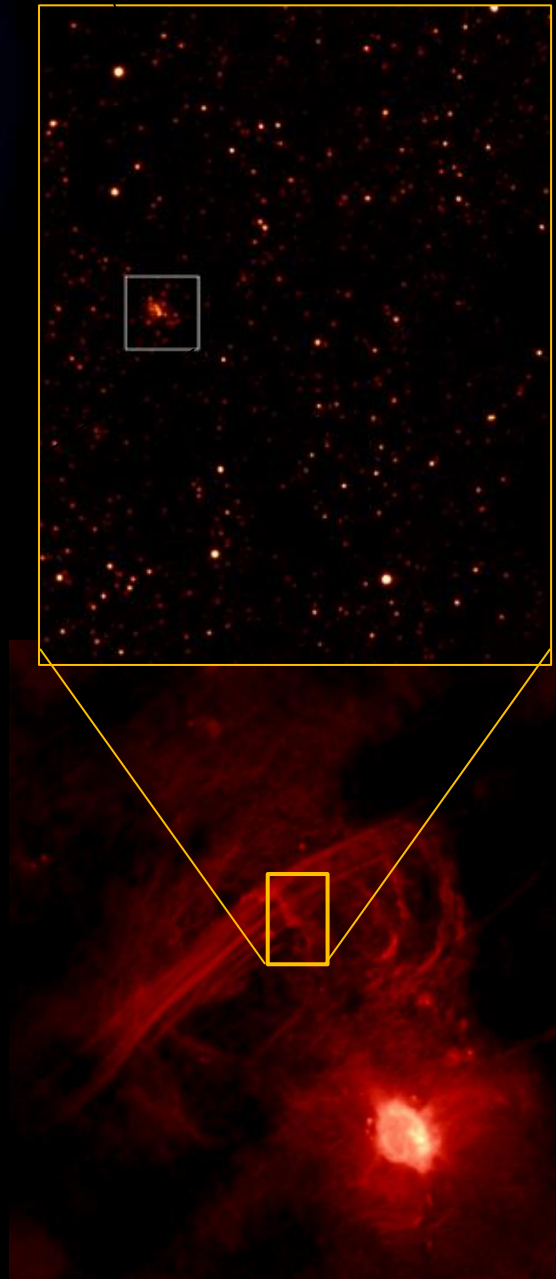
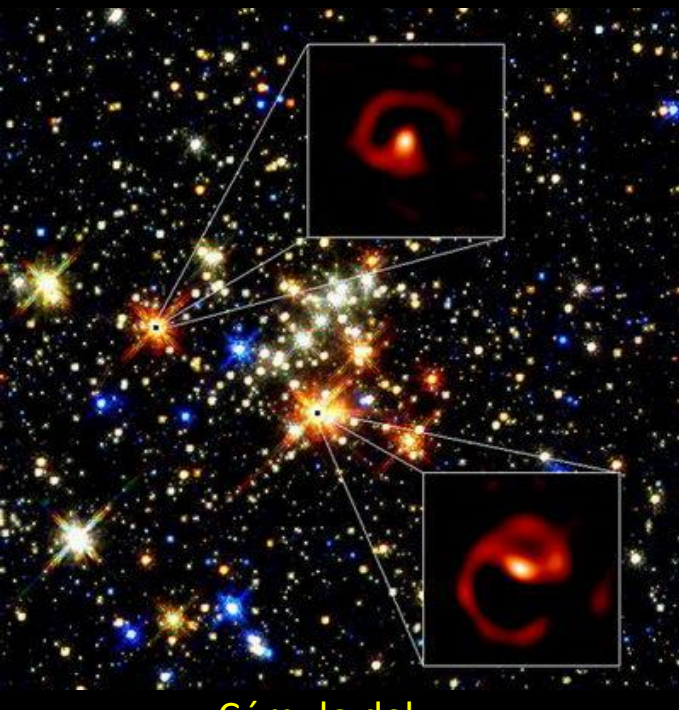
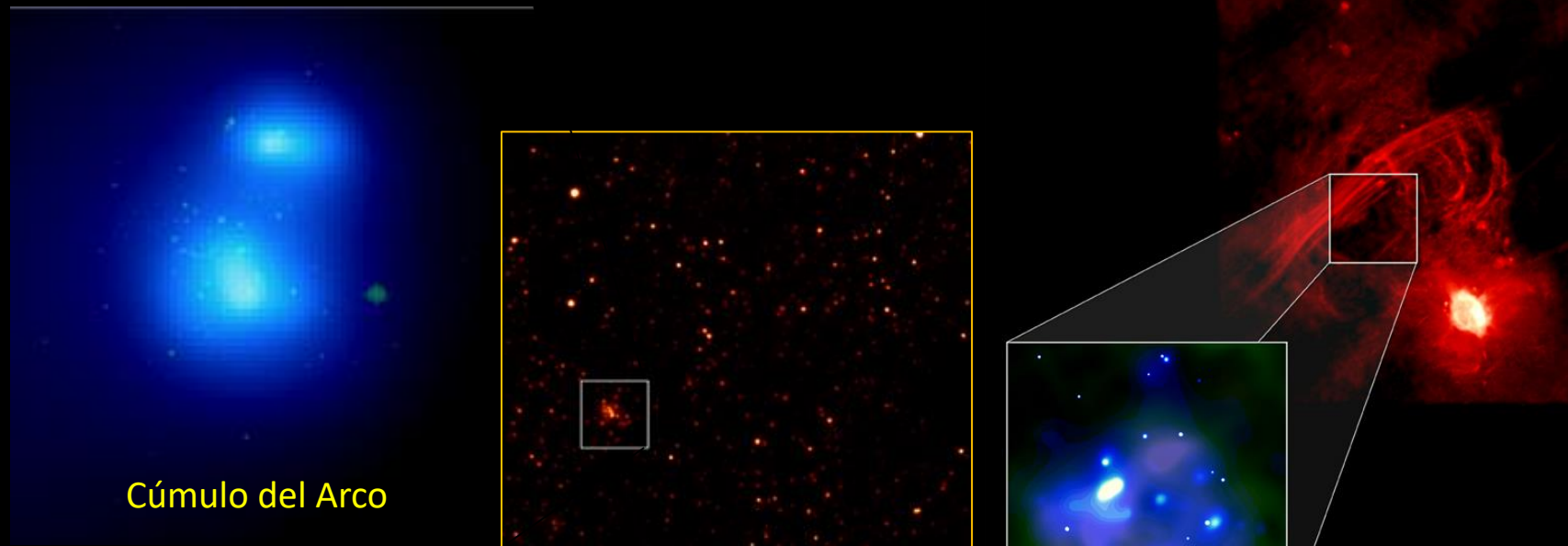
NASA/Spitzer Space Telescope  
Processing: Judy Schmidt

$30' \times 30'$  ( $\sim 80$  pc)

Radio (20cm/1.65 GHz)

NRAO





Nube de gas frío  
del Arco Radio



25'×25'

Rayos-X (azul), IR (verde), Radio (rojo)

Chandra, MSX, VLA



$20' \times 17'$

Rayos-X (3 colores)

Sat. Chandra

Cúmulo del  
Arco

Cúmulo del  
Quintuplo

Nube de gas frío  
del Arco Radio

SgrA

Cúmulo del  
Centro  
Galáctico

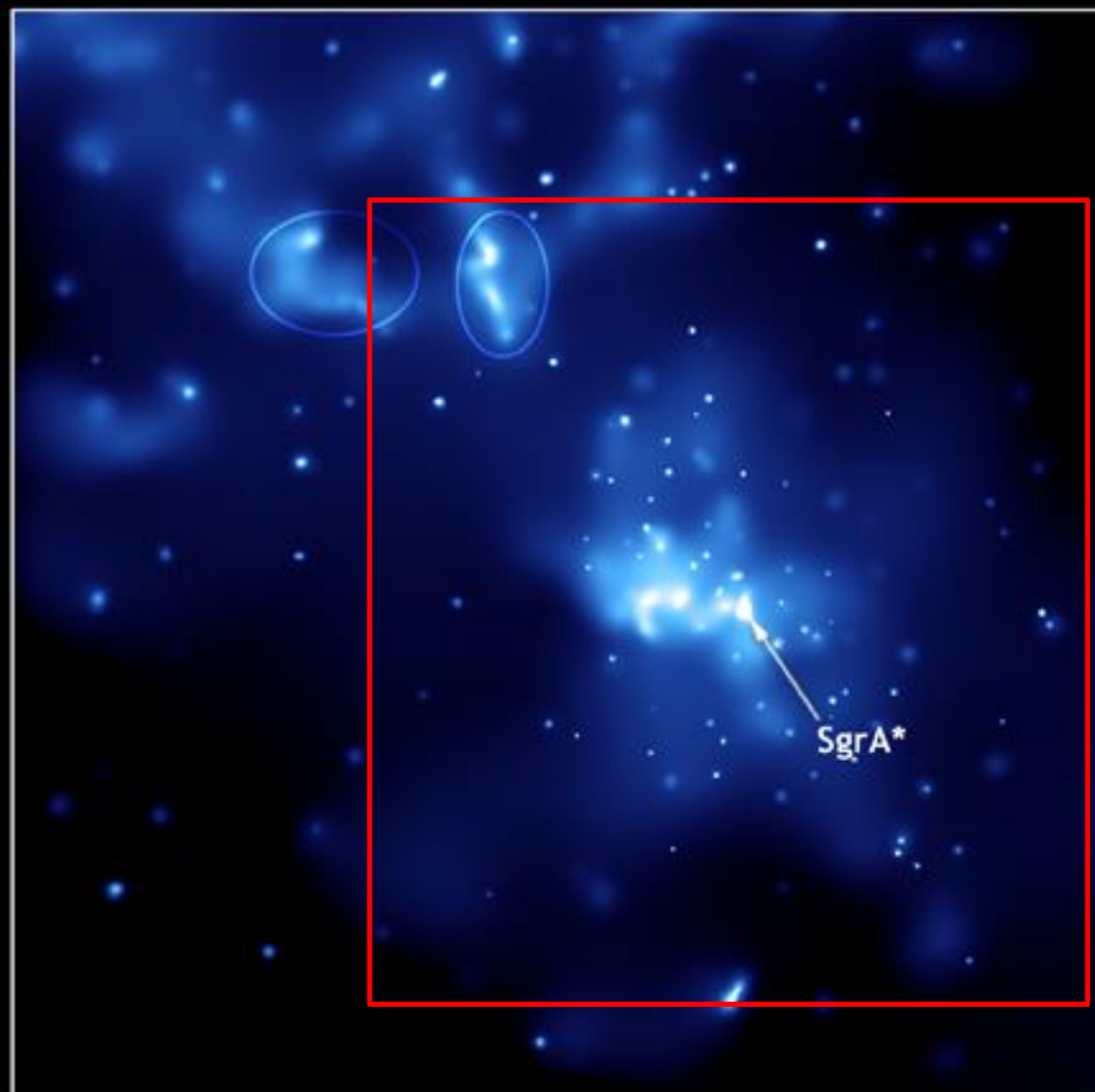
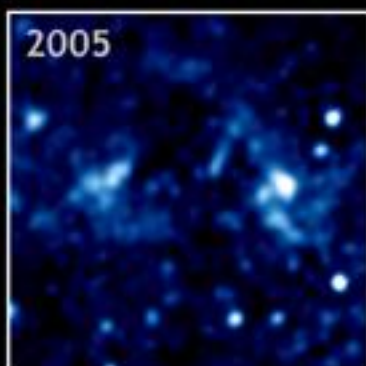
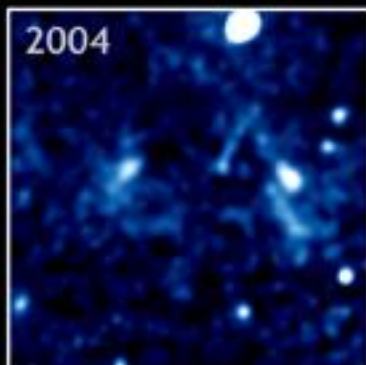
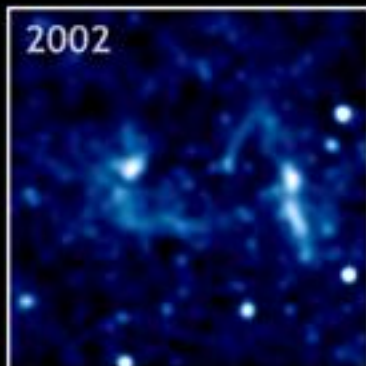




$12.5' \times 12.5'$  ( $\sim 30$  pc)

Rayos-X

Sat. Chandra



$8' \times 8'$  ( $\sim 19$  pc)

Rayos-X (3 colores)

Sat. Chandra

-- Lobe of hot gas --

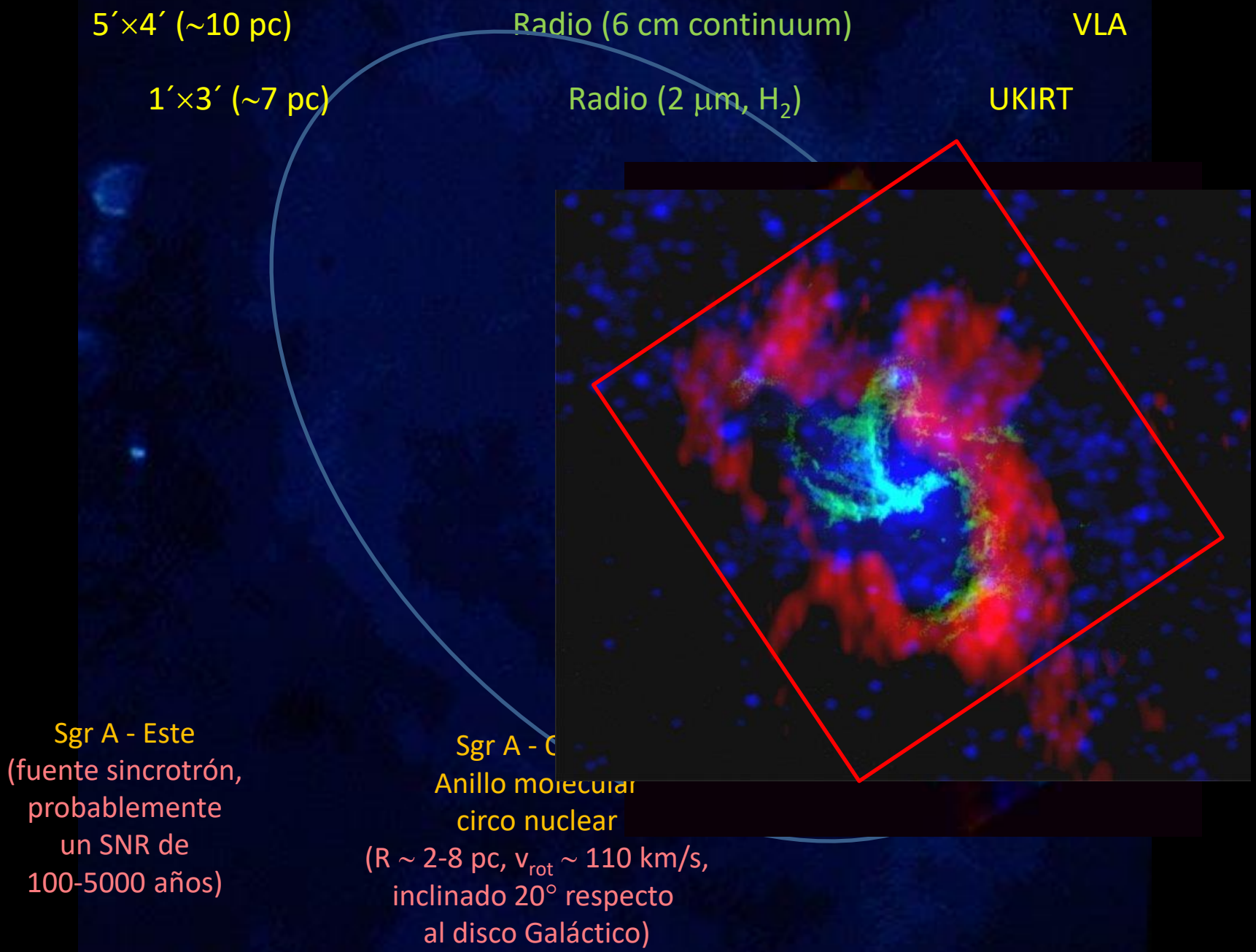
Sgr A\*

-- Lobe of hot gas --

Galactic Plane

SAGITTARIUS A

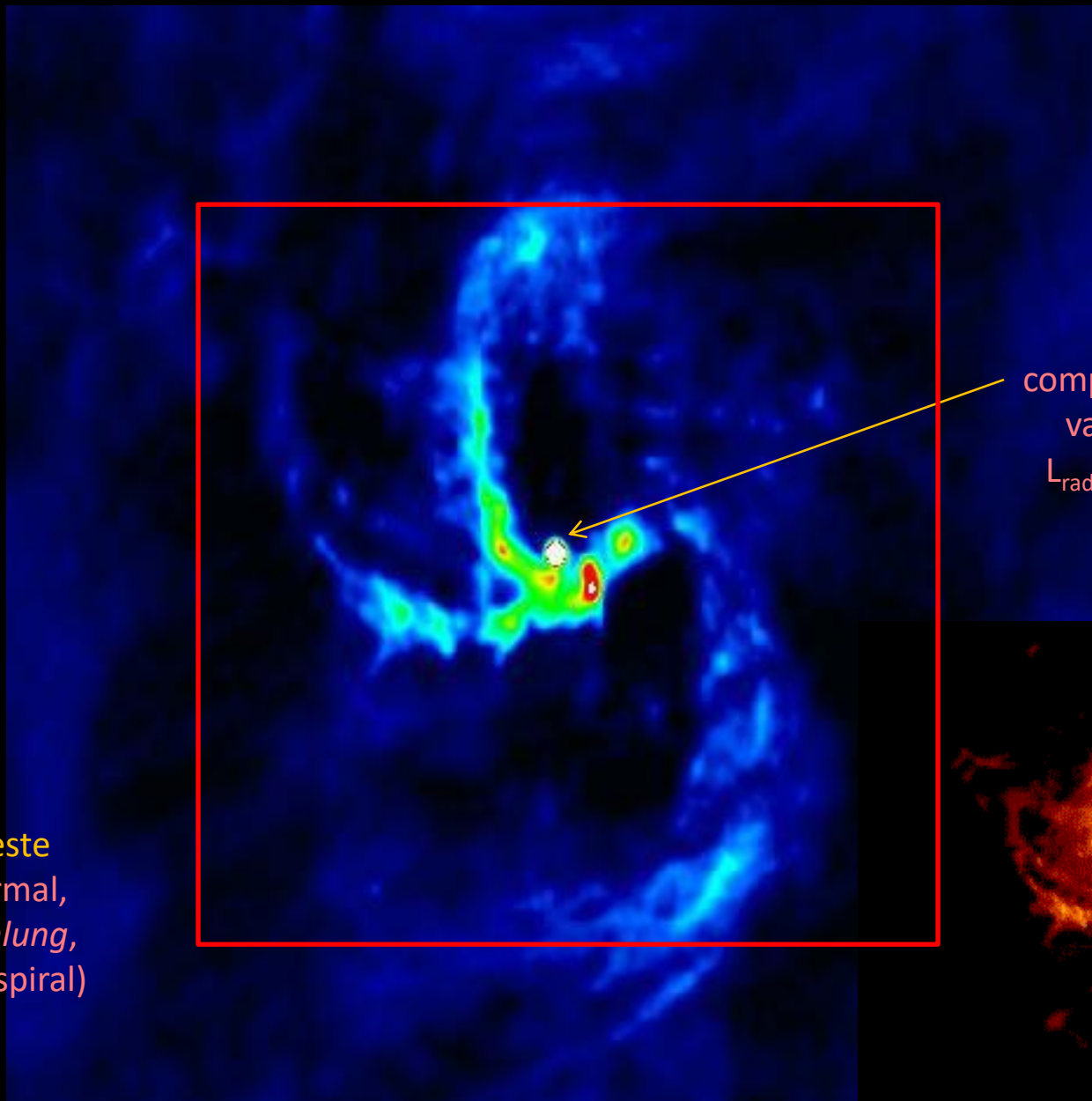




1.7'×1.7'

Radio (3.6 cm)

NRAO



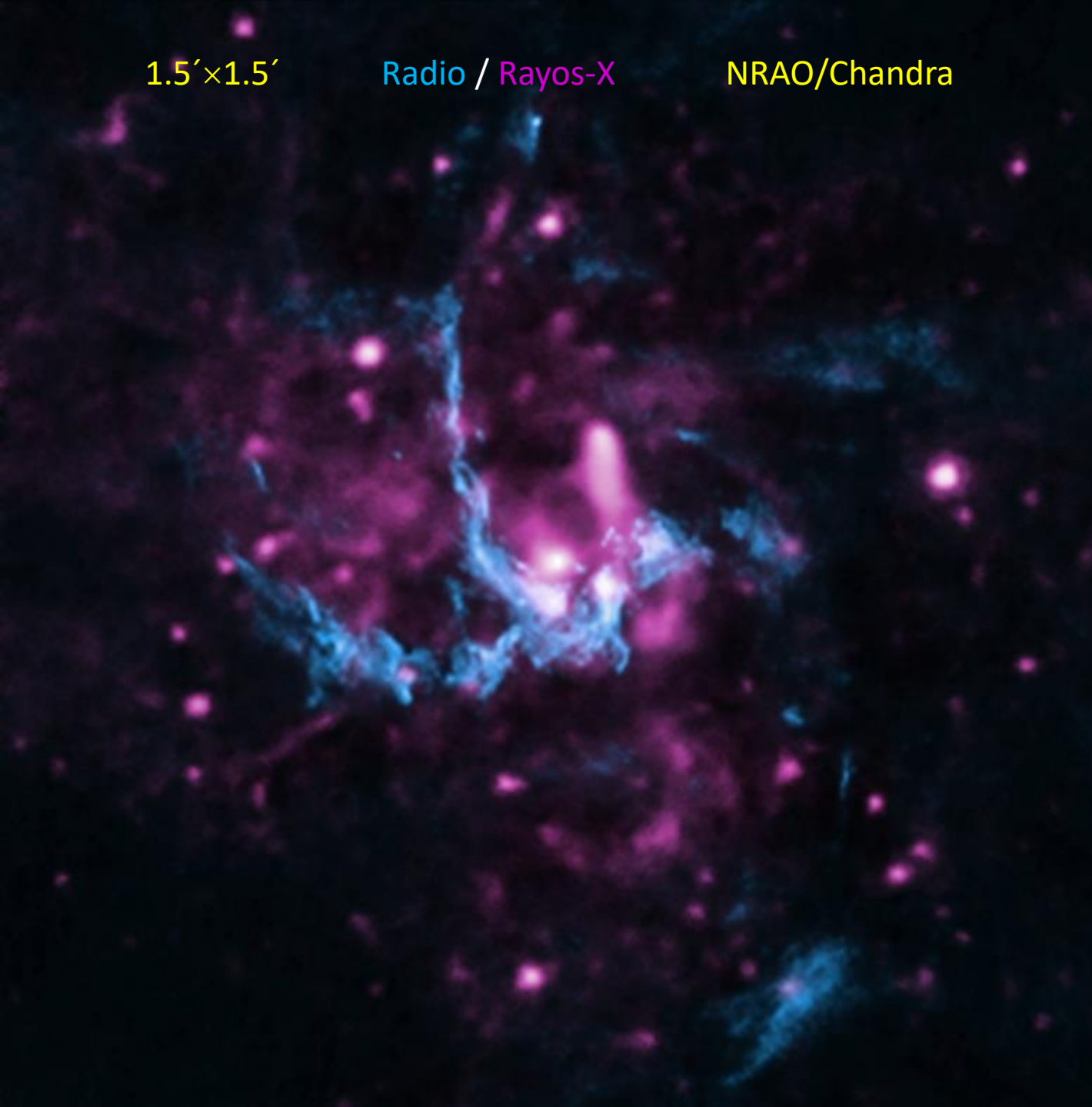
Sgr A - Oeste  
(fuente termal,  
*Bremsstrahlung*,  
región HII espiral)

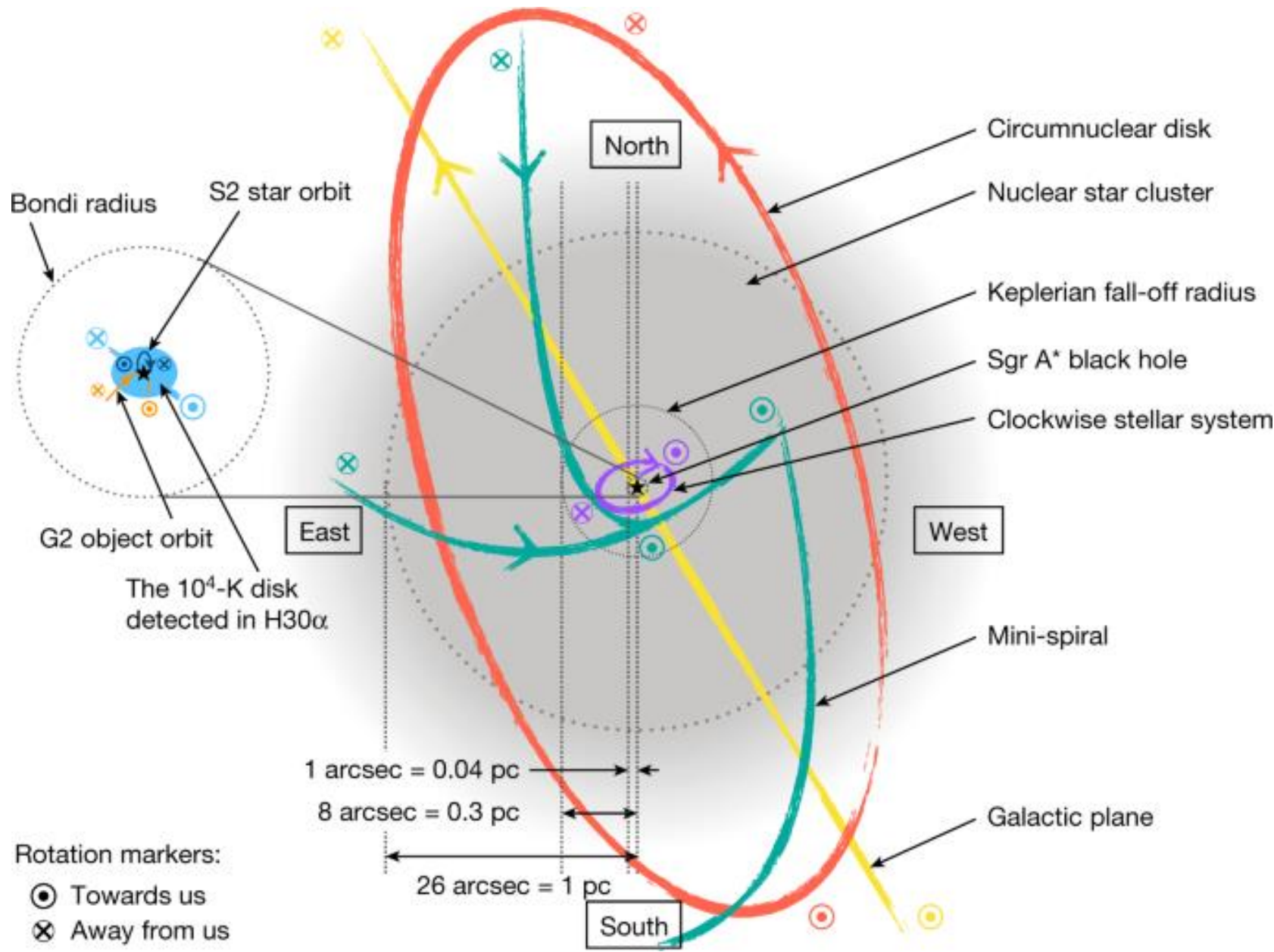
SgrA\*  
(fuente radio  
compacta, no termal,  
variable, < 3 UA,  
 $L_{rad} \sim 2 \times 10^{34}$  erg/s)

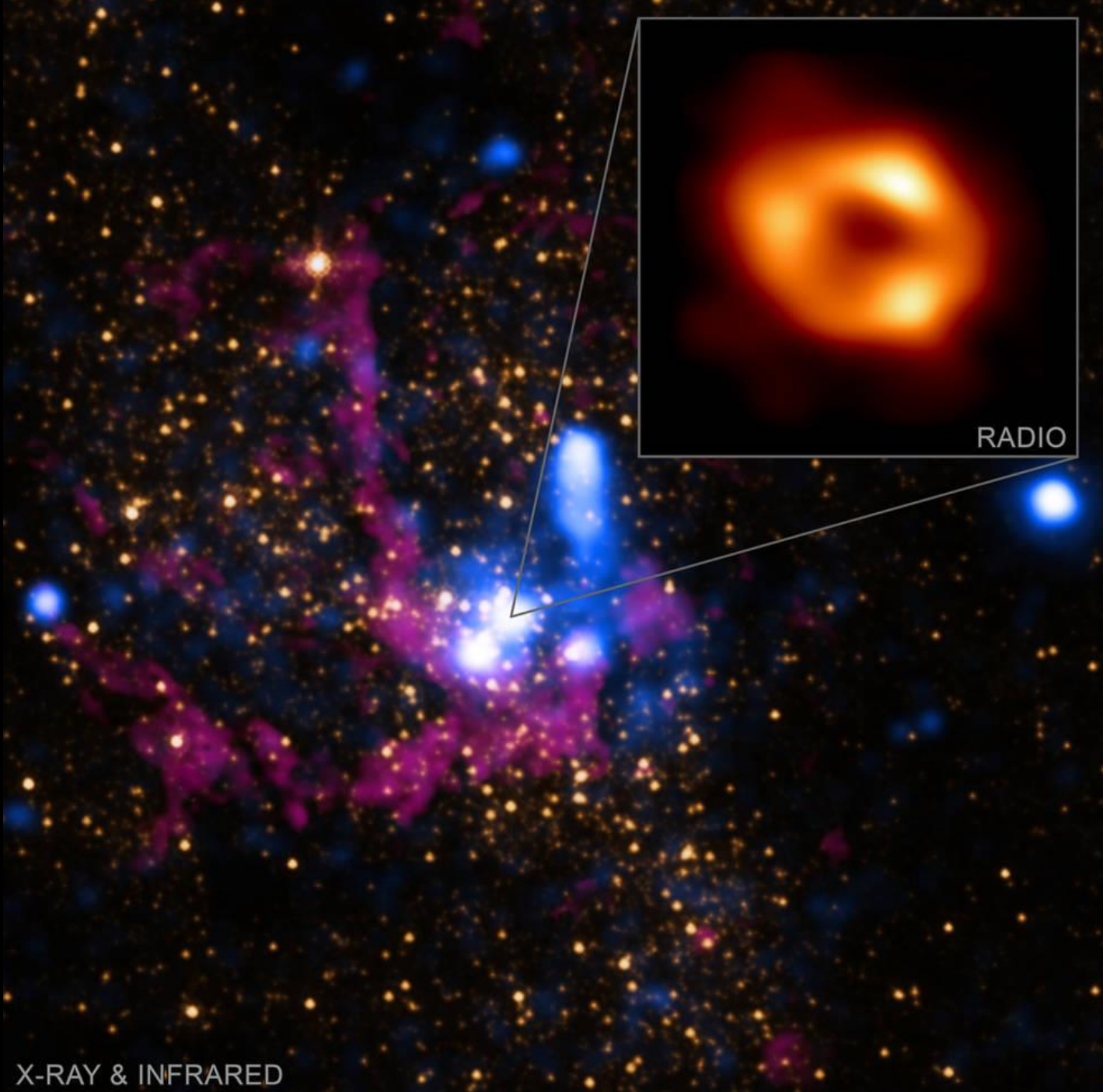
$1.5' \times 1.5'$

Radio / Rayos-X

NRAO/Chandra



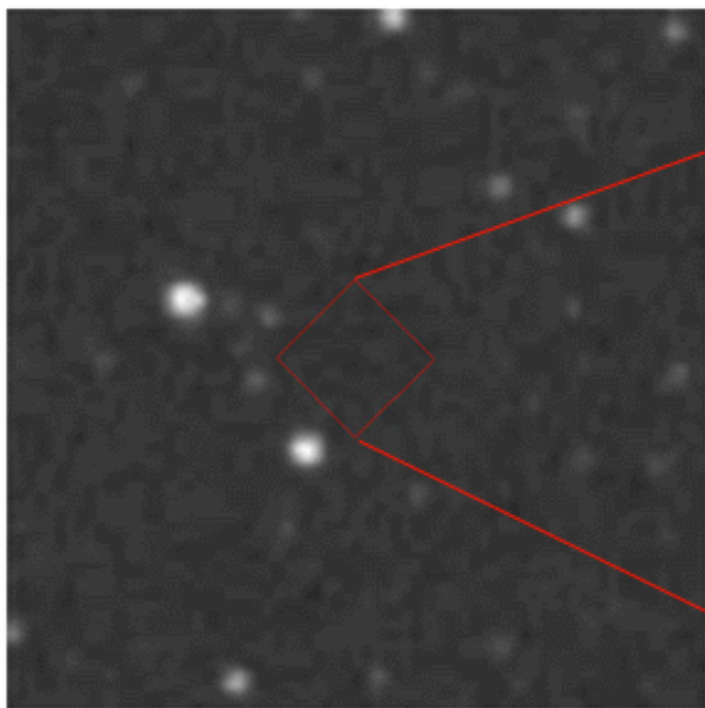




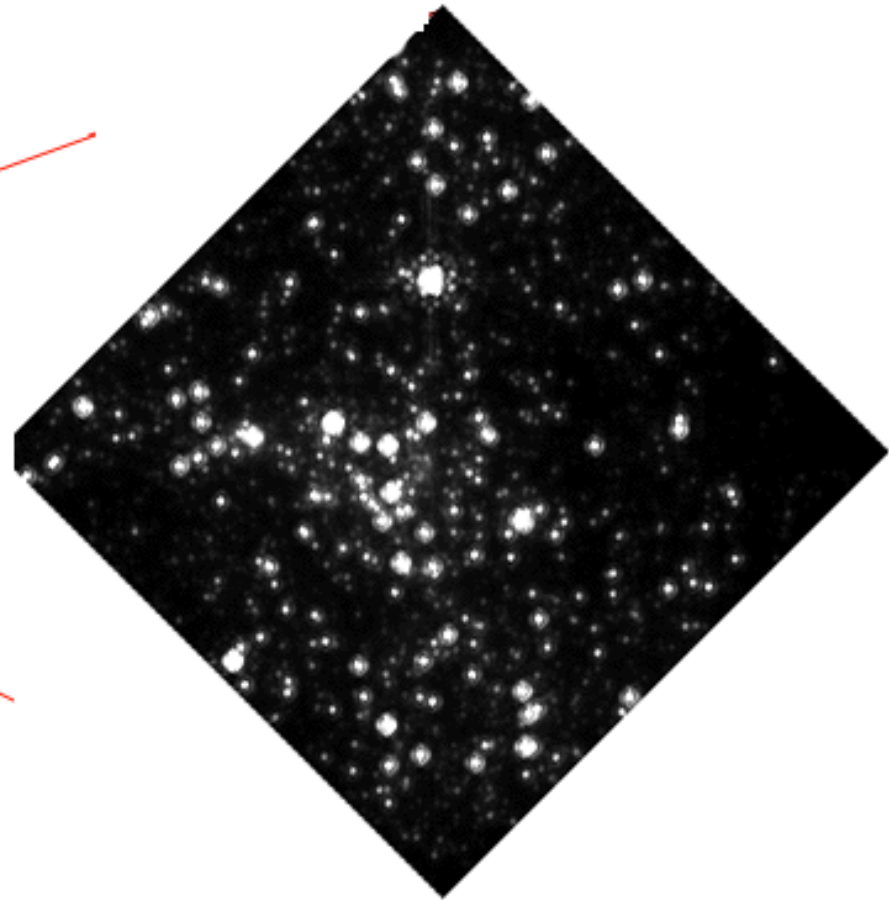
$1' \times 1'$  (2.3 pc)

Óptico/IR

DSS/Blanco (4m)



**Visible Light**



**Infrared Light**

$13'' \times 13''$

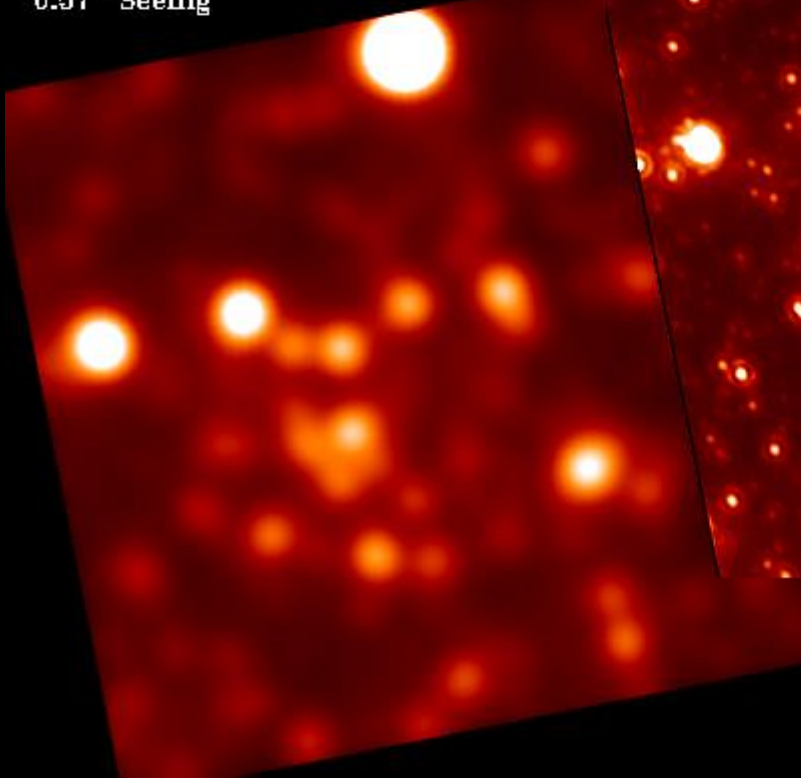
IR (2.2  $\mu\text{m}$ )

Keck (10m)

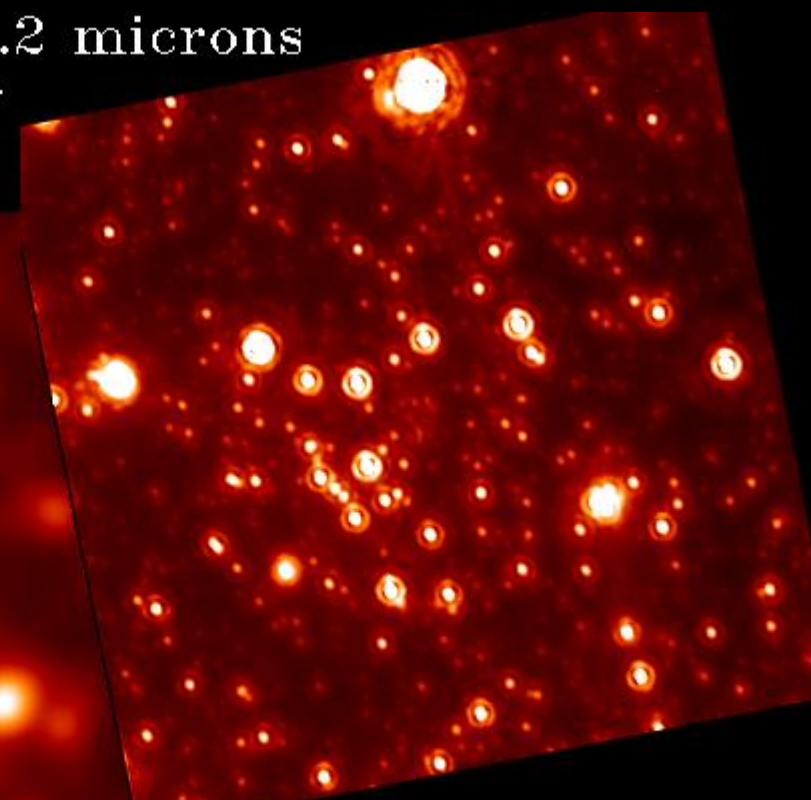
## Galactic Center / 2.2 microns

$13'' \times 13''$  Field. 15 minutes exposure.

Without Adaptive Optics compensation  
0.57'' Seeing



With Adaptive Optics compensation  
0.13'' Full Width at Half Maximum



Copyright CFHT, 1995.

$20'' \times 20''$  ( $\sim 0.8$  pc)

IR (1.6-3.5  $\mu\text{m}$ )

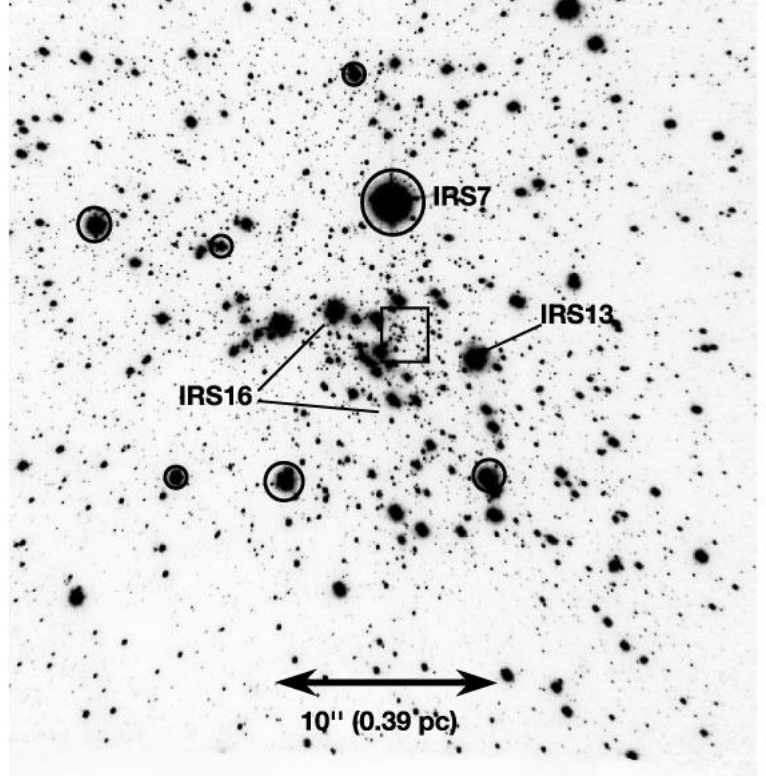
VLT4-Yepun (8.2m)

Cúmulo Compacto  
Central  
 $(R > 1$  pc,  $R_c \sim 0.34$  pc  
gran cantidad de  
estrellas B de la SP  
 $\Rightarrow$  cúmulo joven?  
 $n \propto r^{-1.8} \Rightarrow \sim$  isotermal,  
pero  $\sigma$  crece en  
dirección al centro!)

movimientos  
propios  
(mas de 1,000 estrellas  
dentro de un radio de  
 $10''$  de Sgr A\*)



a K<sub>s</sub>-band

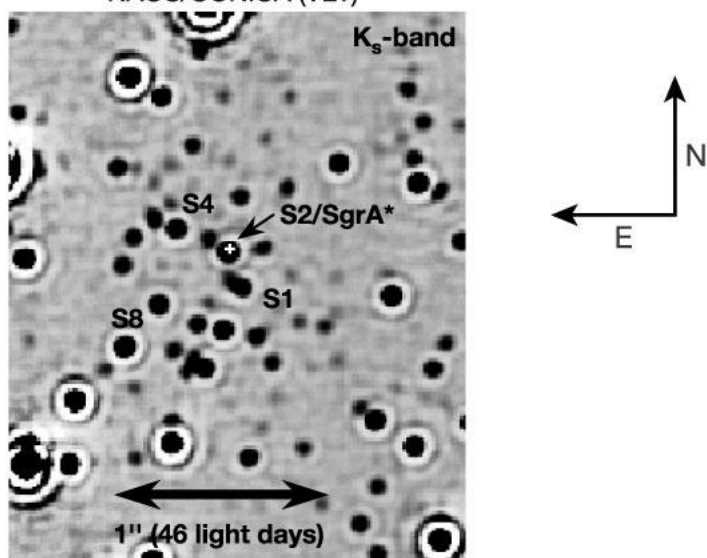


IR (2.1  $\mu$ m)

VLT4-Yepun (8.2m)

movimientos propios +  
velocidades radiales  
(~ 20 estrellas  
dentro de un radio de  
5'' de Sgr A\*)

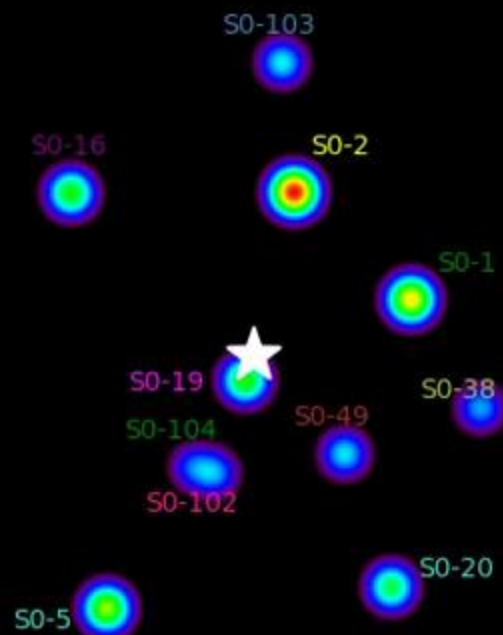
b



1992      10 light days

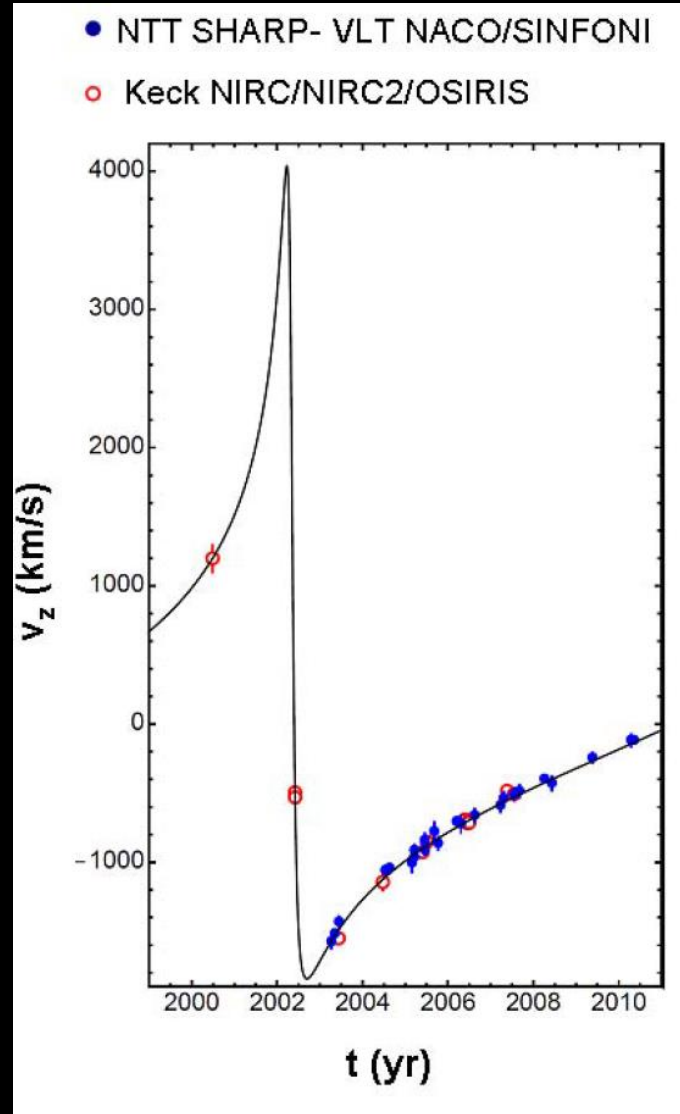
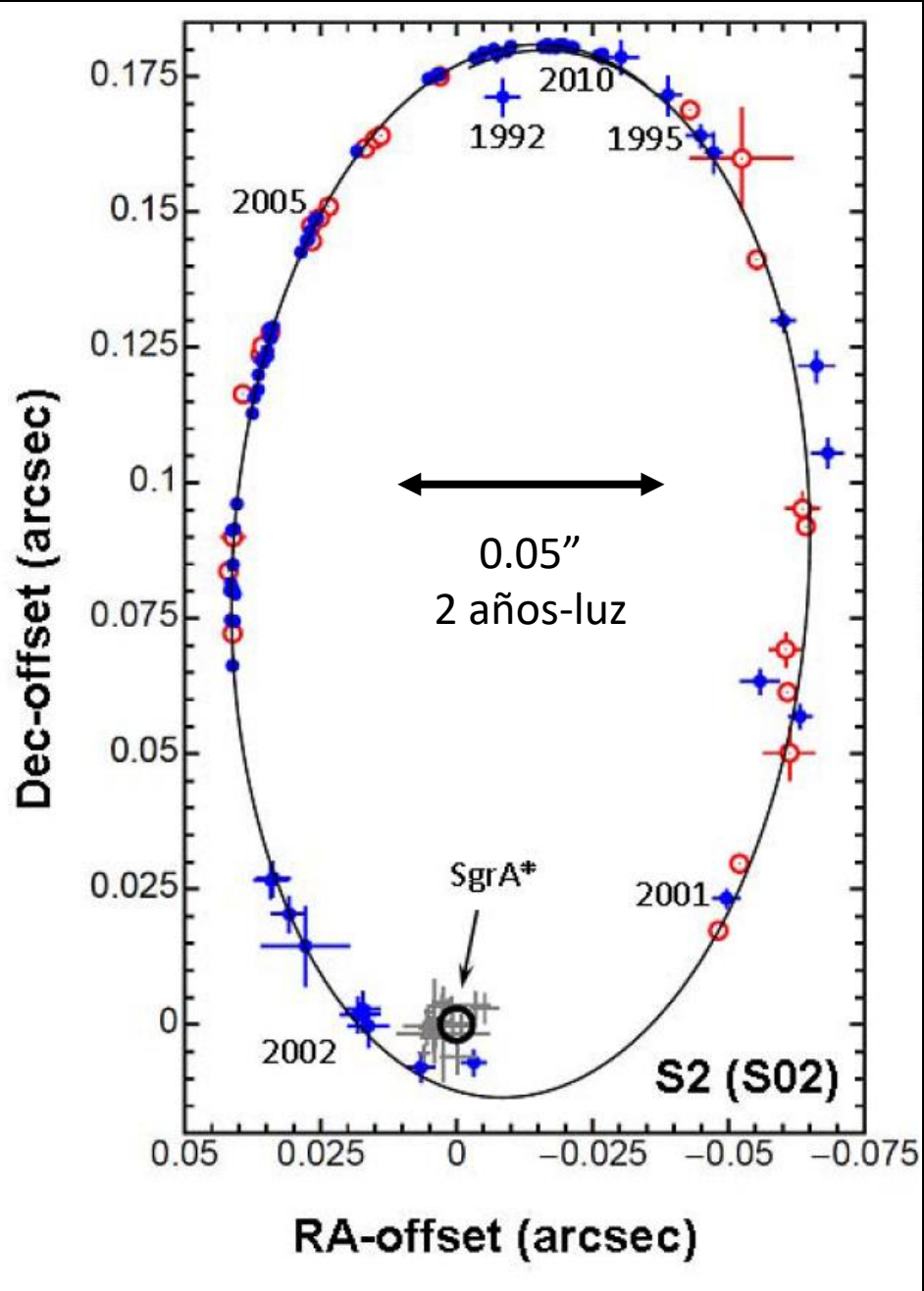


**1995.5**

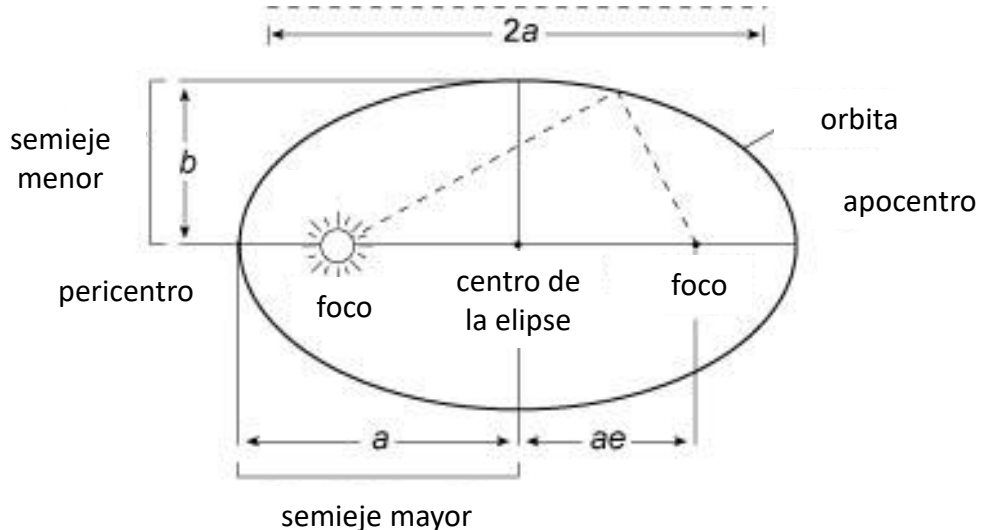


**0.1"**

**Keck/UCLA Galactic  
Center Group**



## S2



**S2**  
 $(\epsilon = 0.87, P = 15.2 \text{ años},$   
 pericentro = 120 UA,  
 velocidad máxima  $\sim 5000 \text{ km/s}$ )

### ★ pericentro y apocentro

$$r_{\text{peri}} = a - ae = a (1 - e)$$

$$r_{\text{apo}} = a (1 + e)$$

### ★ 3<sup>a</sup>. Ley de Kepler

$$P^2 = (4 \pi^2) / [G (M+m)] a^3$$

$$\left. \begin{aligned} a &= r_{\text{peri}} / (1 - e) \\ a &= 120 / (1 - 0.87) = 923.08 \text{ UA} \end{aligned} \right.$$

$$\left. \begin{aligned} M &\sim (4 \pi^2 a^3) / (G P^2) \\ M &= [4 \pi^2 (923.08)^3] / [39.484 (15.2)^2] \\ &= 3.4 \times 10^6 M_{\odot} \end{aligned} \right.$$

$$\begin{aligned} G &= 6.673 \times 10^{-11} \text{ N m}^2 \text{ kg}^{-2} = 6.673 \times 10^{-11} \text{ m}^3 \text{ s}^{-2} \text{ kg}^{-1} \\ &= 6.673 \times 10^{-11} (1.495979 \times 10^{11})^{-3} (3.155815 \times 10^7)^2 (1.9891 \times 10^{30})^1 \text{ UA}^3 \text{ año}^{-2} M_{\odot}^{-1} \\ G &= 39.484289 \text{ UA}^3 \text{ año}^{-2} M_{\odot}^{-1} \end{aligned}$$

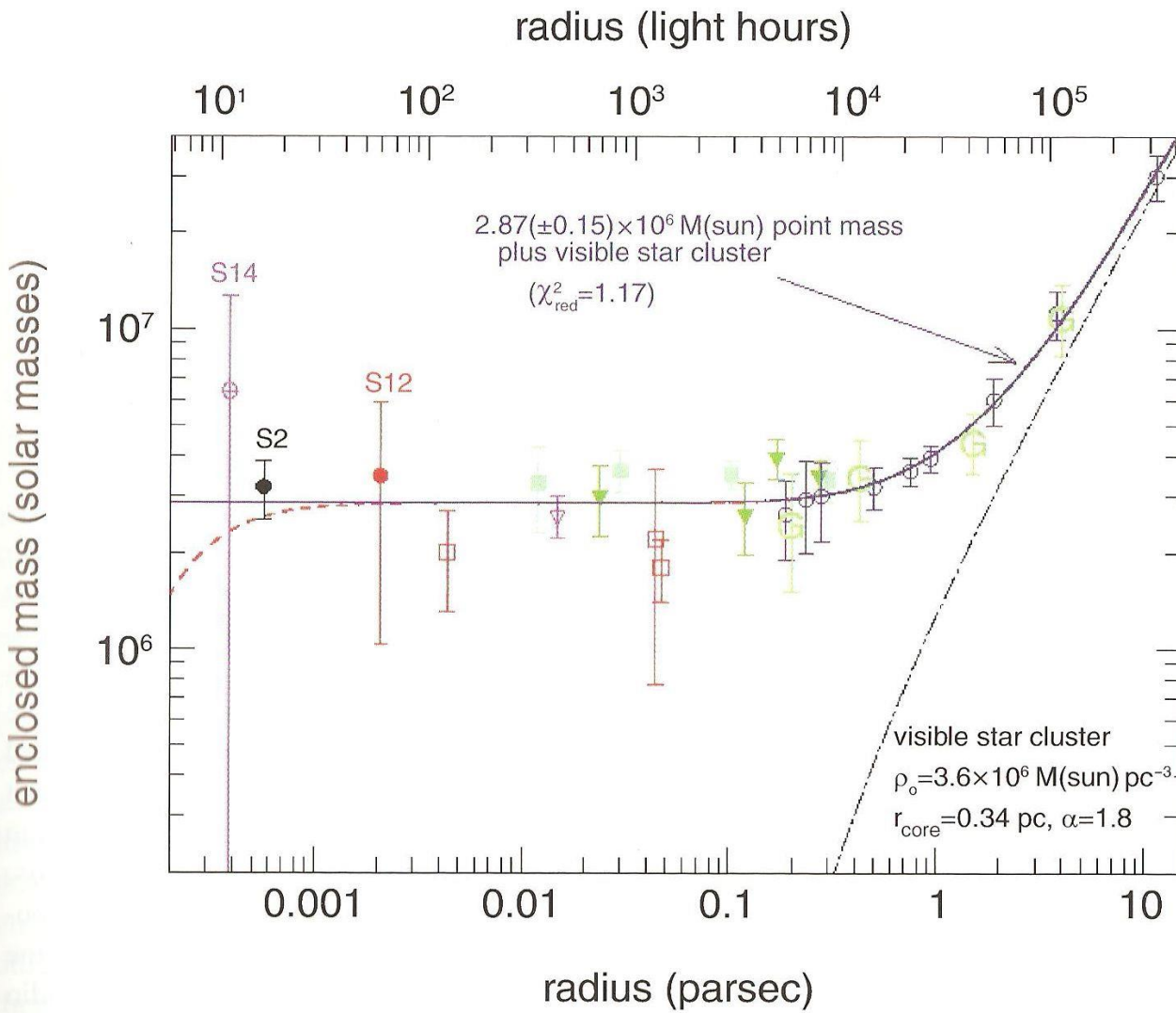
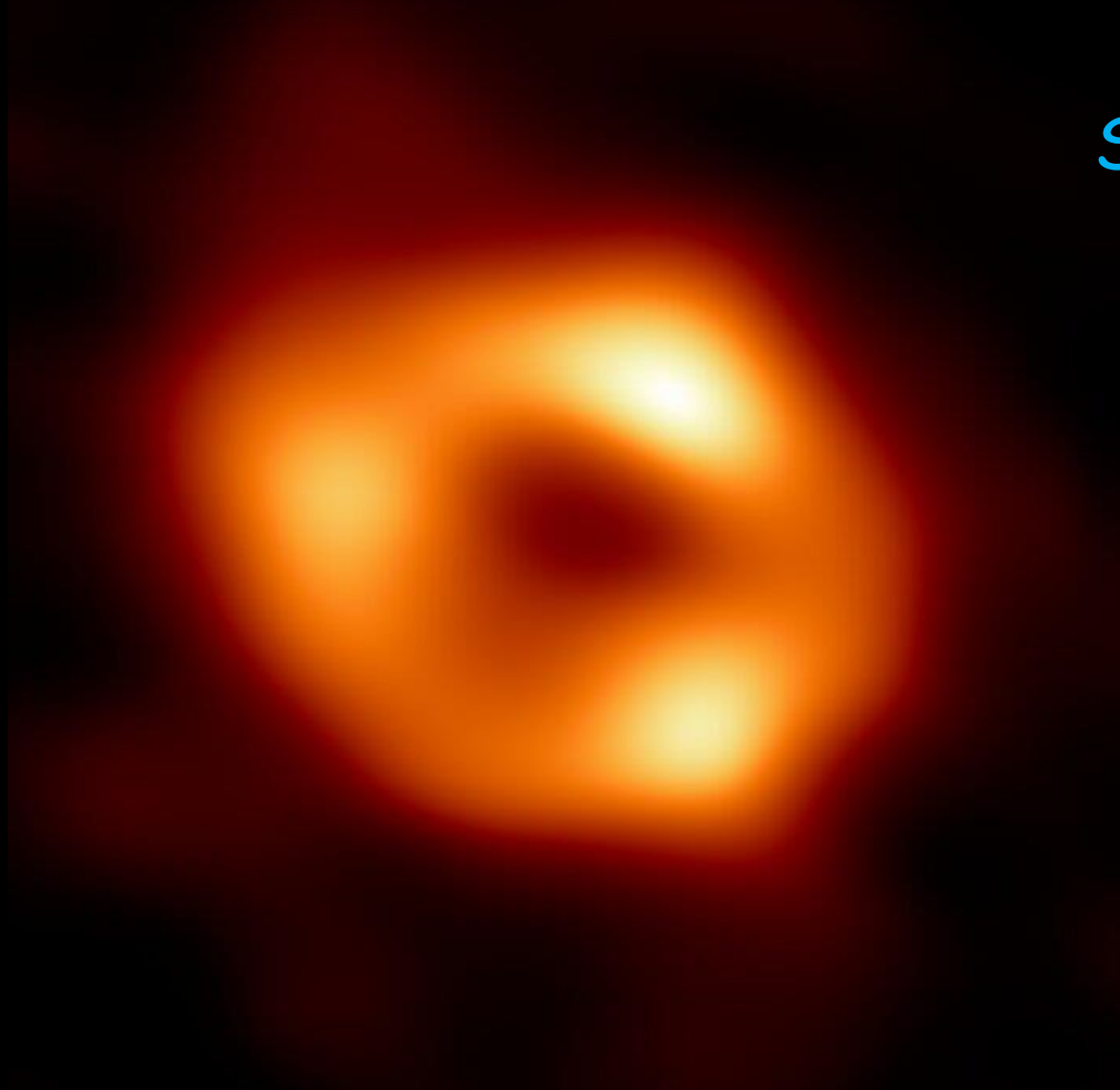


**Fig. 2.38.** Determination of the mass  $M(r)$  within a radius  $r$  from  $\text{Sgr A}^*$ , as measured by the radial velocities and proper motions of stars in the central cluster. Mass estimates obtained from individual stars (S14, S2, S12) are given by the points with error bars for small  $r$ . The other data points were derived from the kinematic analysis of the observed proper motions of the stars, where different methods have been applied. As can be seen, these methods produce results that are mutu-

ally compatible, so that the mass profile plotted here can be regarded to be robust. The solid curve is the best-fit model, representing a point mass of  $2.9 \times 10^6 M_\odot$  plus a star cluster with a central density of  $3.6 \times 10^6 M_\odot/\text{pc}^3$  (the mass profile of this star cluster is indicated by the dash-dotted curve). The dashed curve shows the mass profile of a hypothetical cluster with a very steep profile,  $n \propto r^{-5}$ , and a central density of  $2.2 \times 10^{17} M_\odot \text{ pc}^{-3}$ .

Sgr A\*



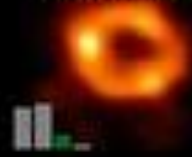
average 1



average 2



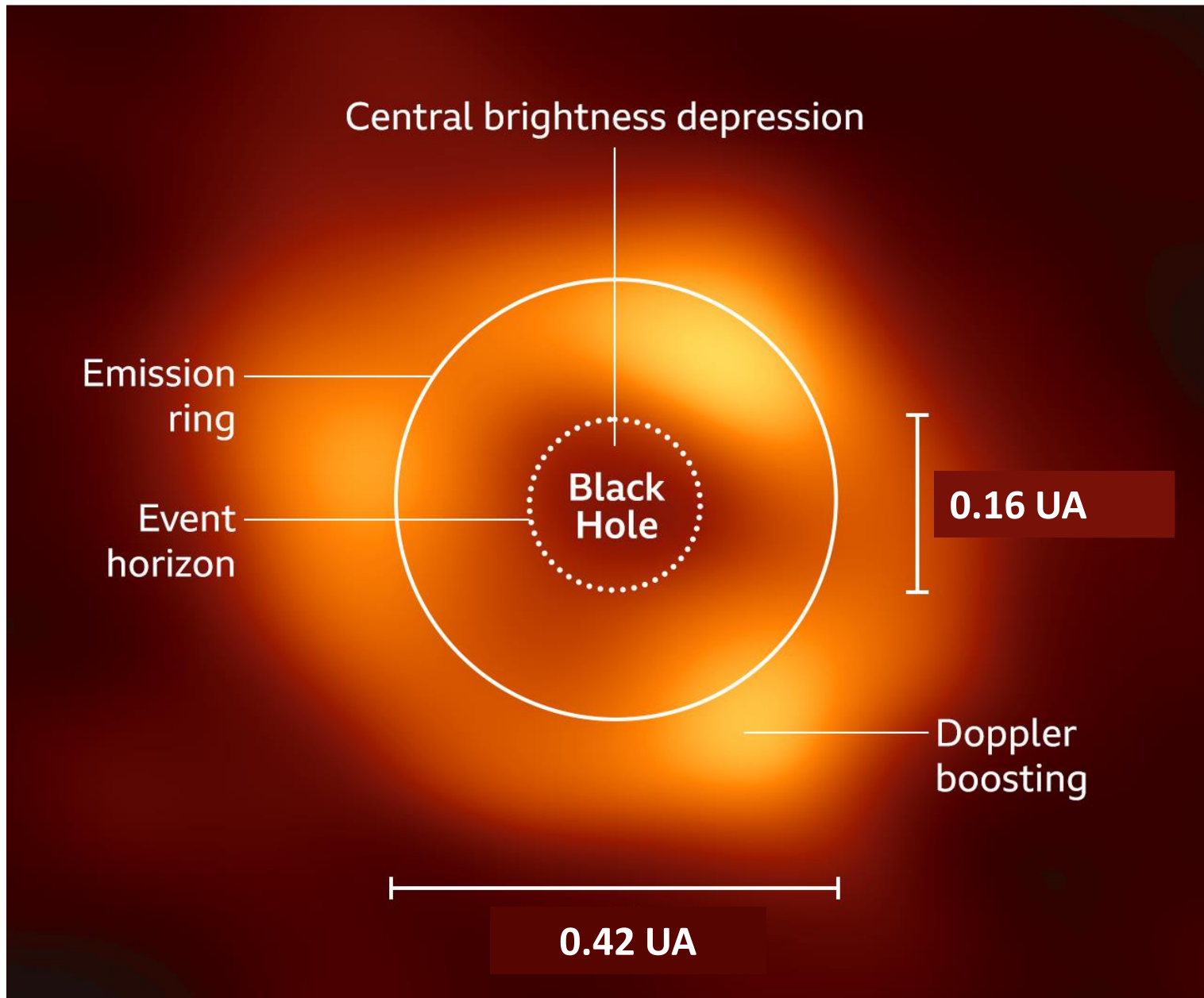
average 3

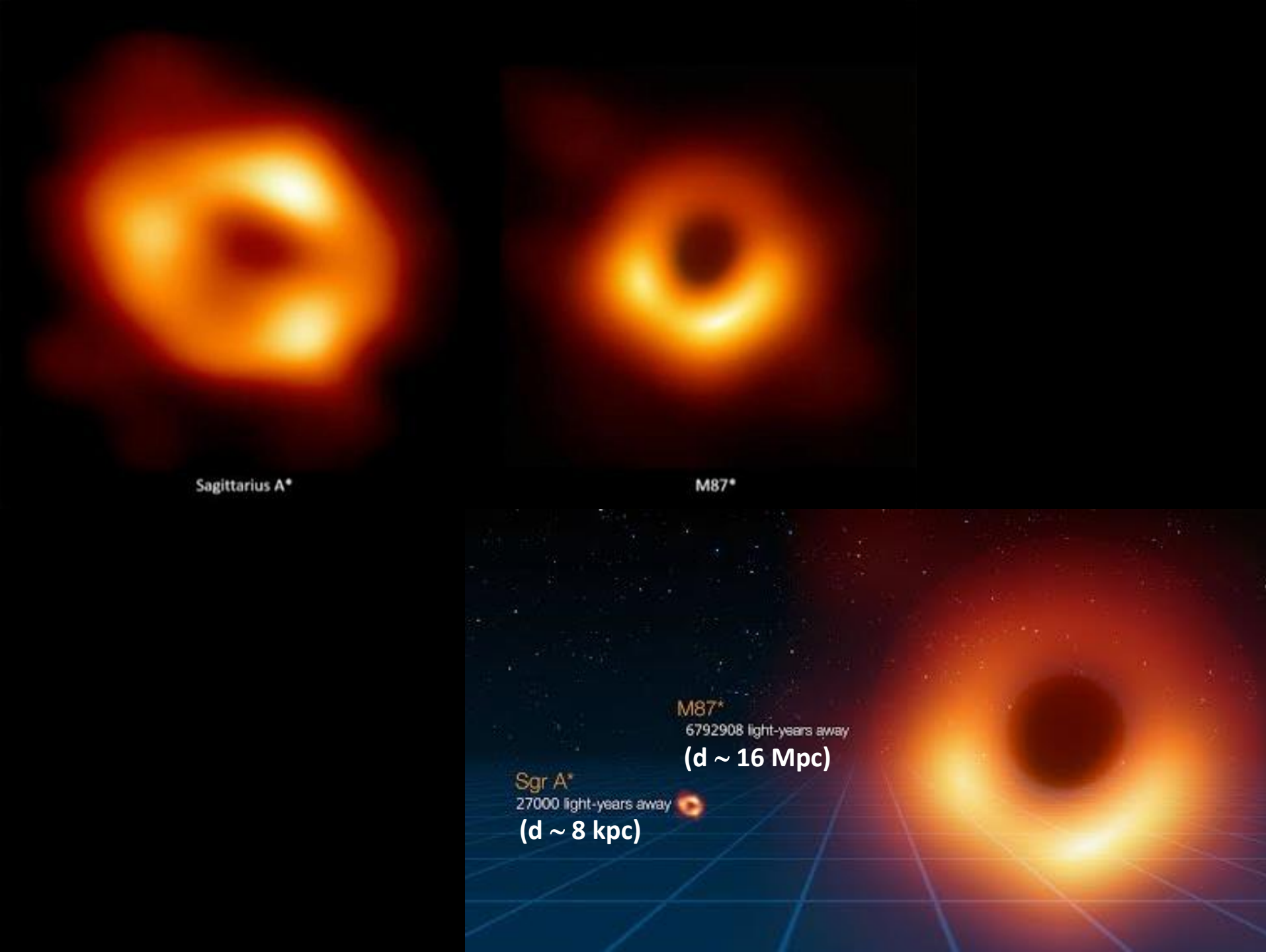


average 4



# Deciphering the image of Sagittarius A\*





Sagittarius A\*

M87\*

M87\*

6792908 light-years away

( $d \sim 16$  Mpc)

Sgr A\*

27000 light-years away

( $d \sim 8$  kpc)

M87\*

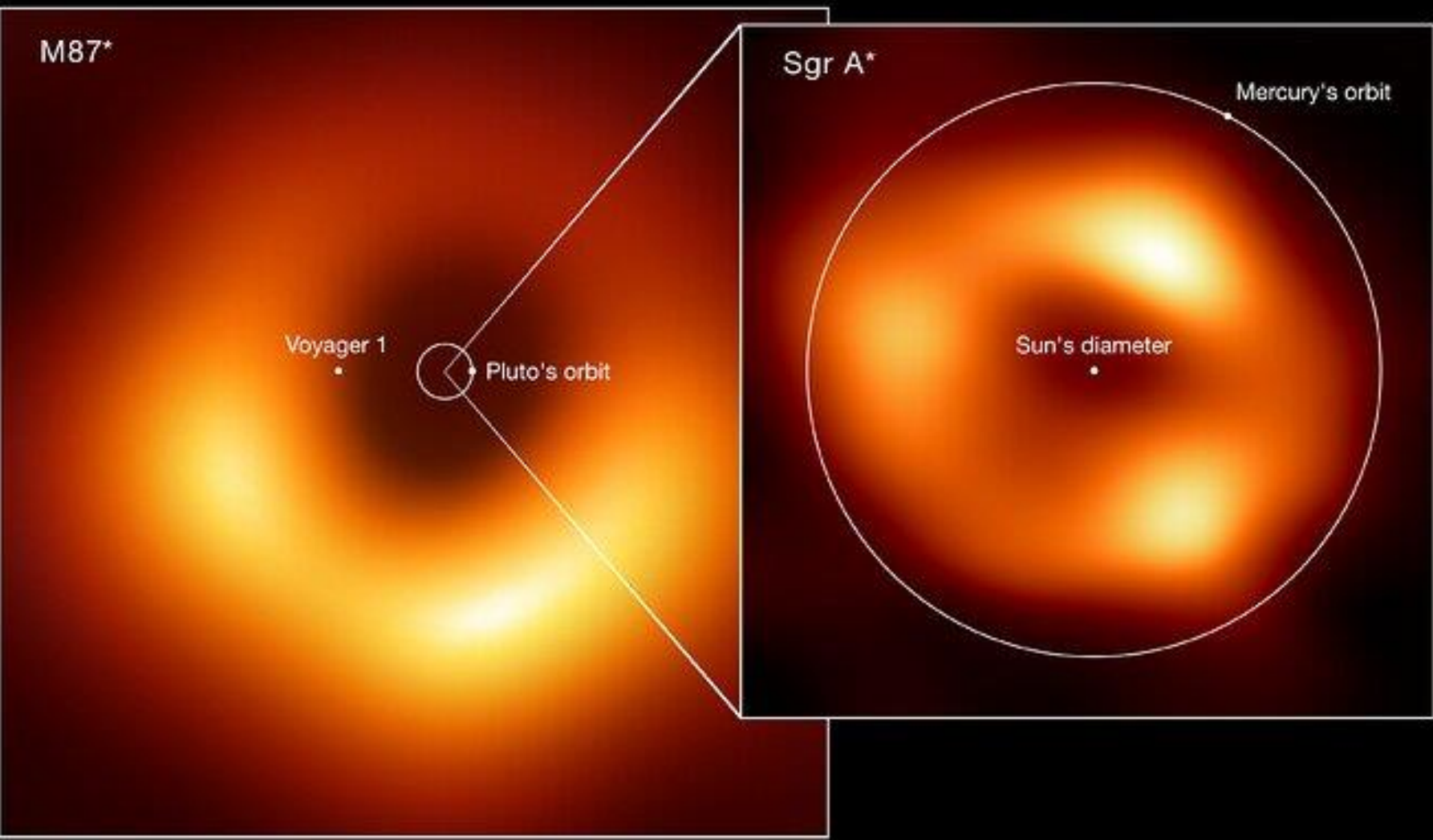
Voyager 1

Pluto's orbit

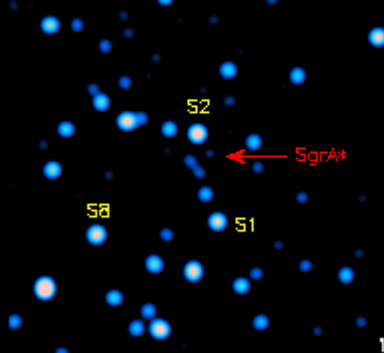
Sgr A\*

Sun's diameter

Mercury's orbit

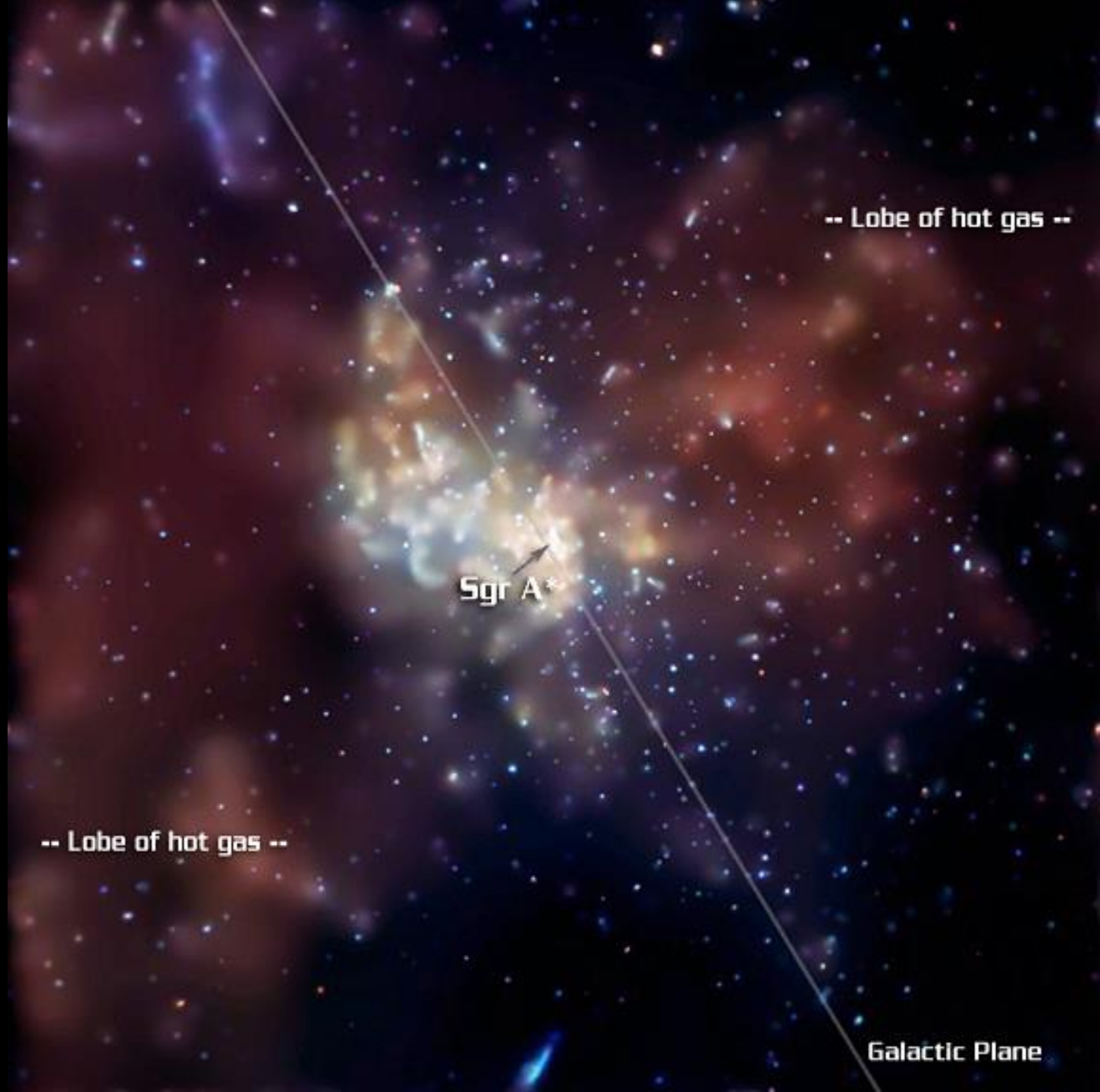


20 light days



### Flares

rayos-X ( $T \sim$  horas), NIR ( $1.7 \mu\text{m}$ ,  $T \sim 17^{\text{min}}$ ), 1.3 mm ( $T \sim$  horas)  
[*Chandra*, XMM, NuSTAR]      [VLT *Yepun*]      [VLBI]  
 $\Rightarrow$  tamaño  $< 10^8 \text{ km}$  (0.7 UA)

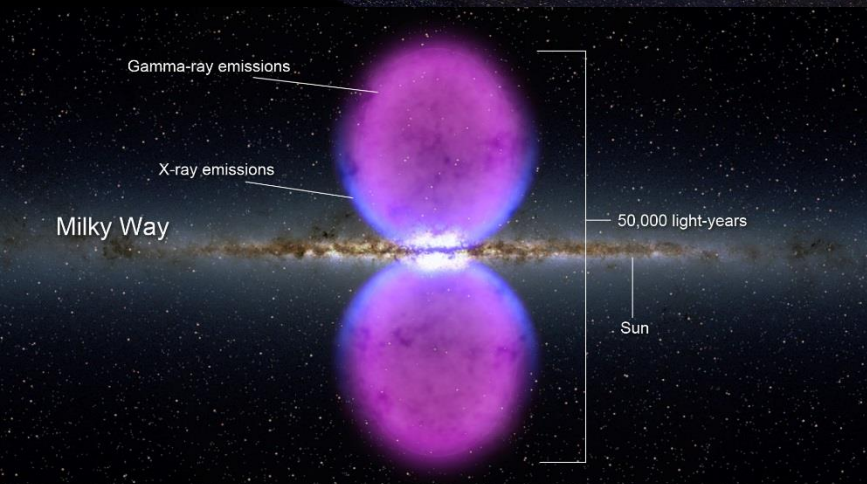
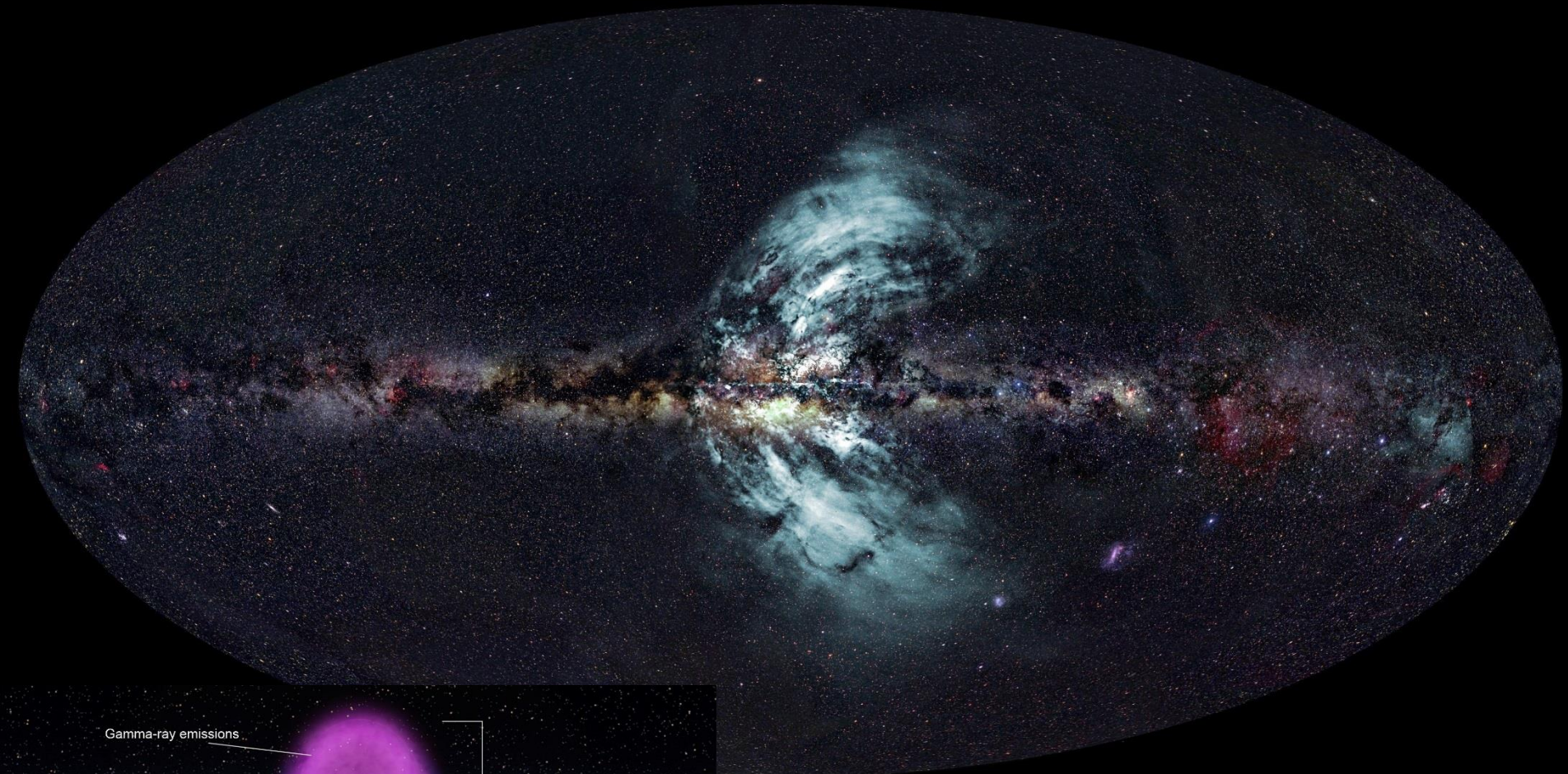


-- Lobe of hot gas --

Sgr A\*

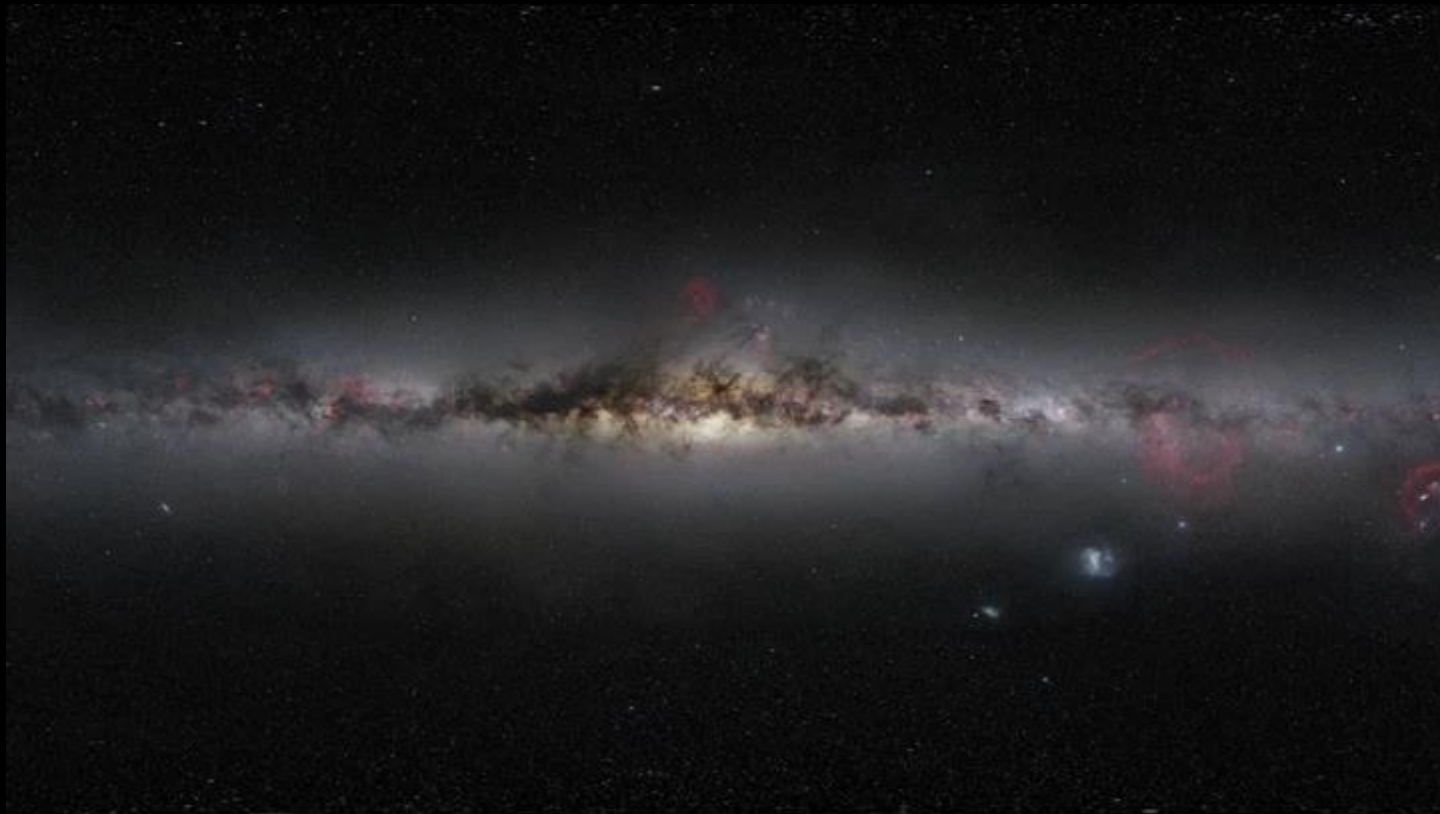
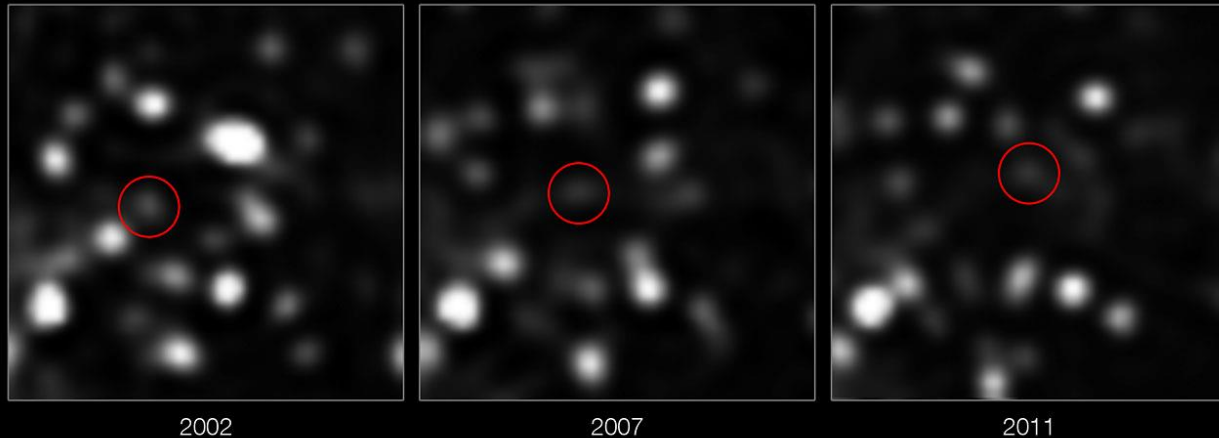
-- Lobe of hot gas --

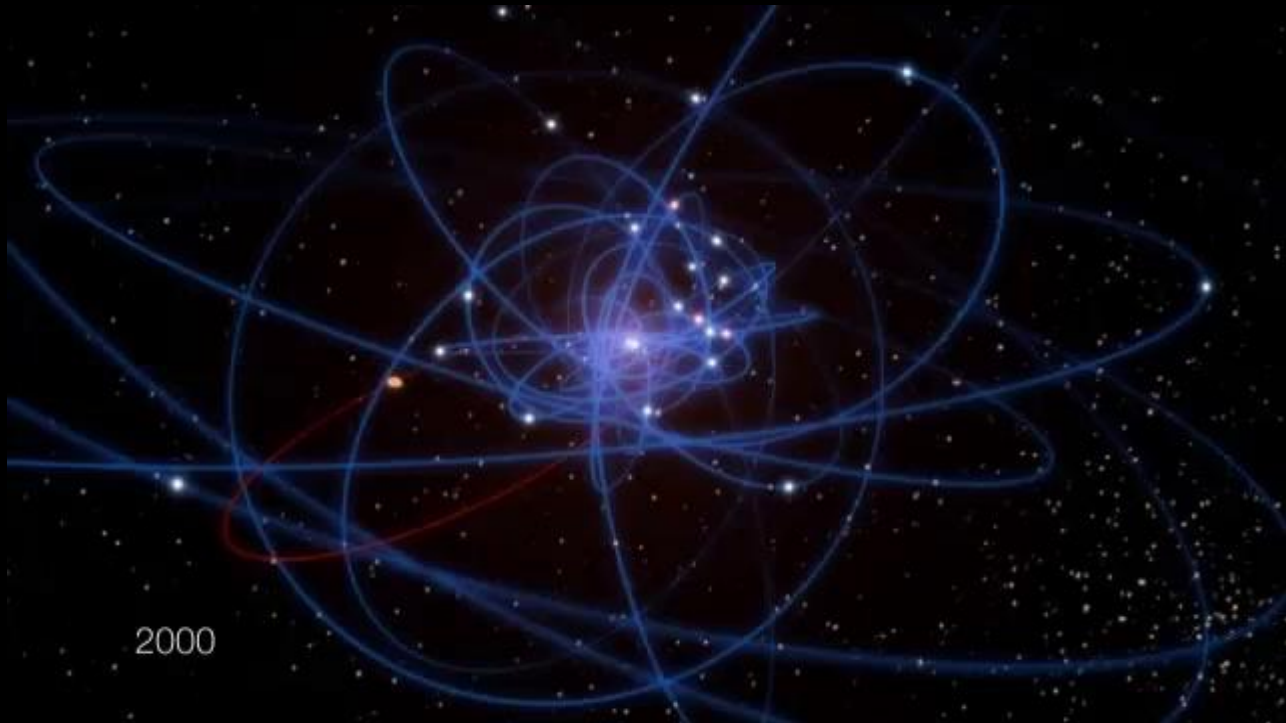
Galactic Plane

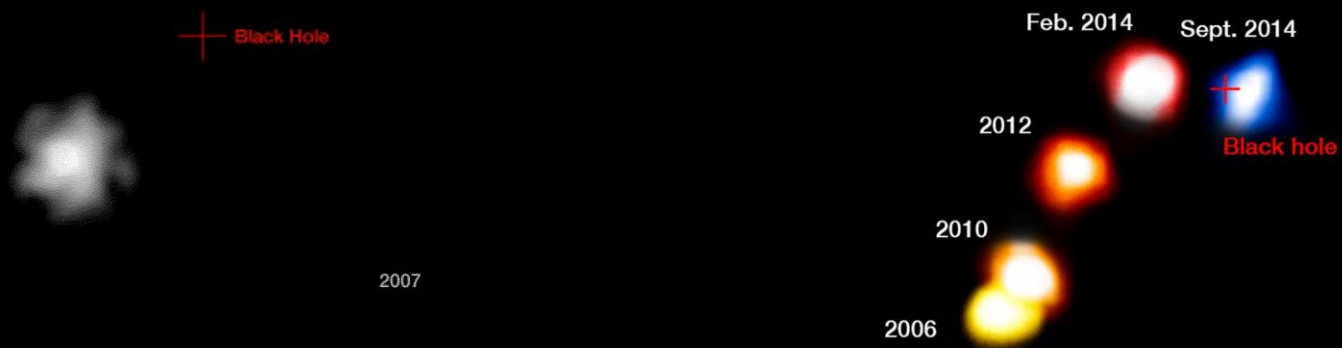


*Burbujas de Fermi*

*G2: Nebulosa suicida!? ( $\sim 3 M_{\odot}$ )*  
Máximo acercamiento: 2013-2014





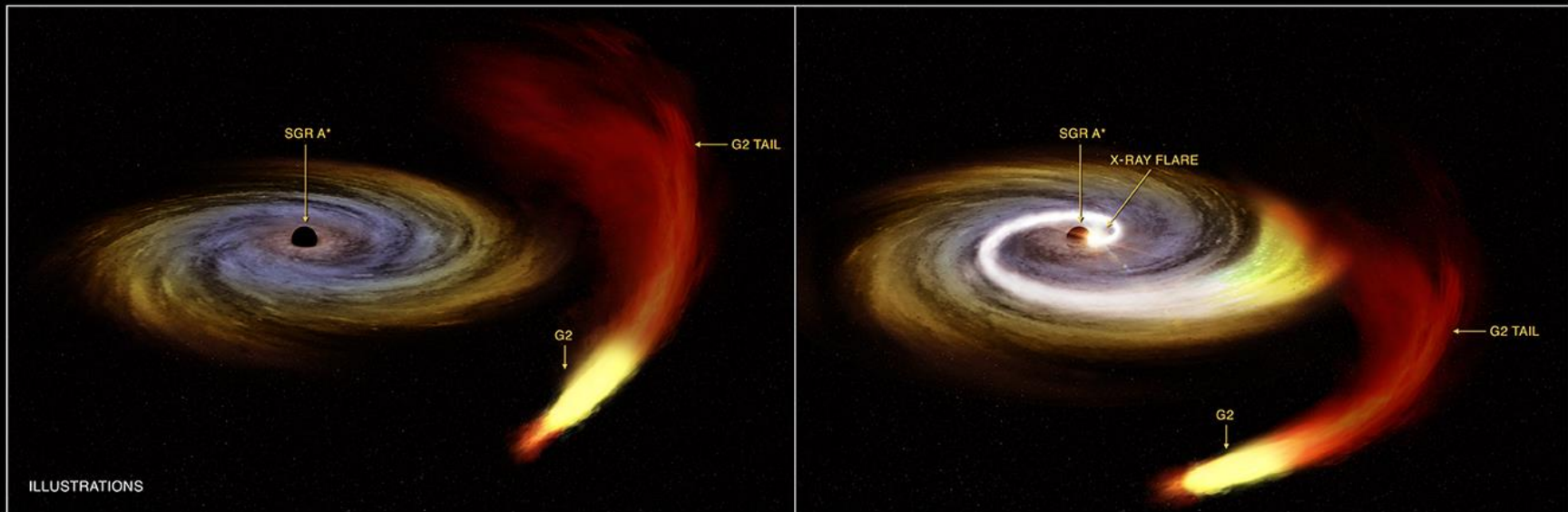


*G2*

$V_{\text{before}} = 9,700 \text{ km/h}$

$V_{\text{after}} = 12,000 \text{ km/h}$

$R_{\text{peri}} = 270 \text{ UA} (\text{predicted})$



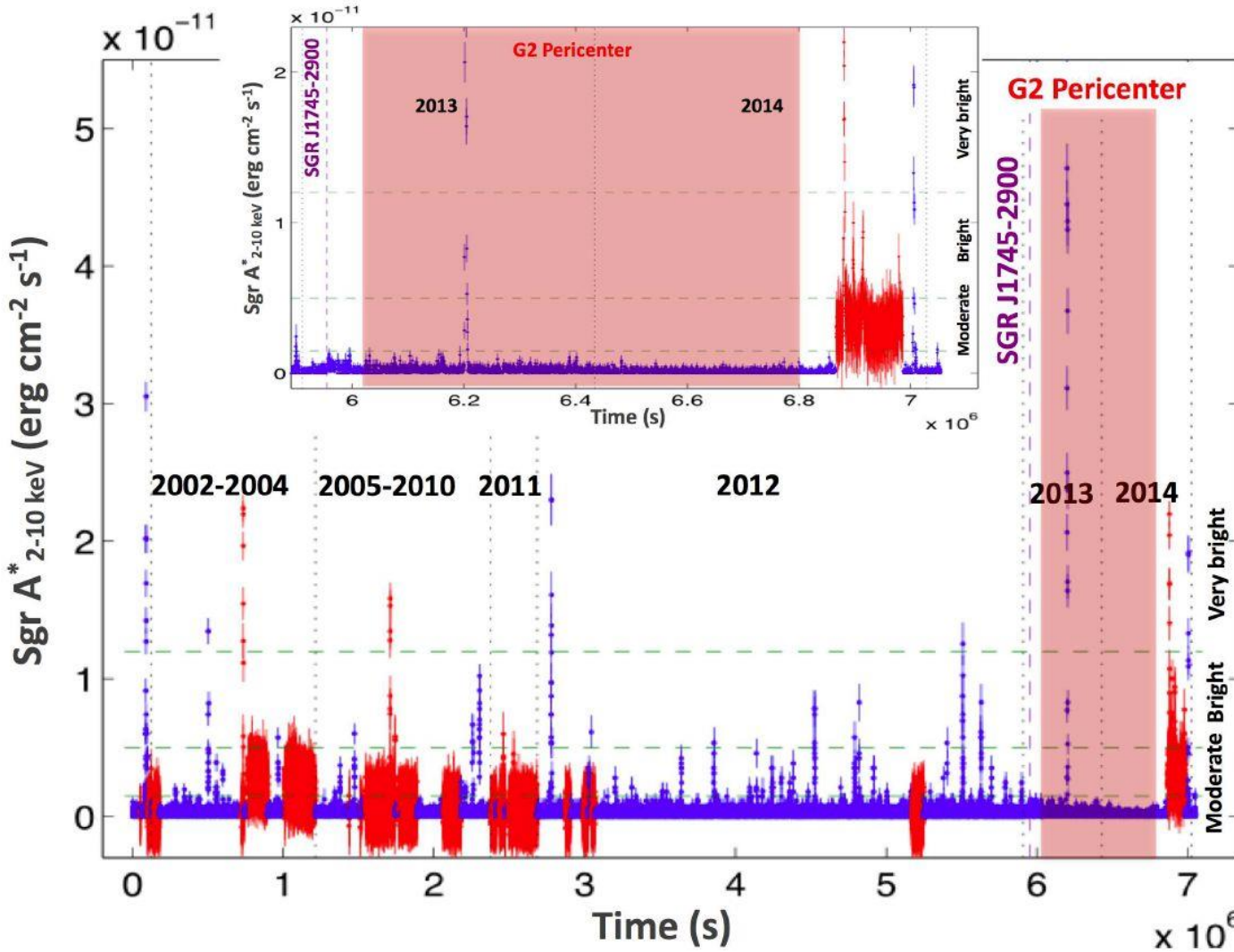
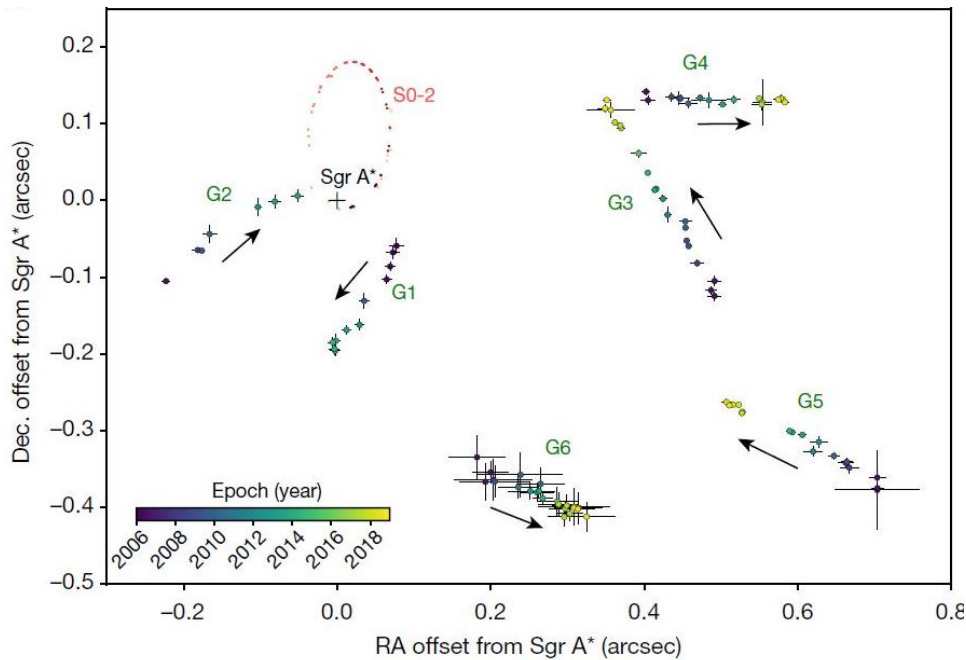


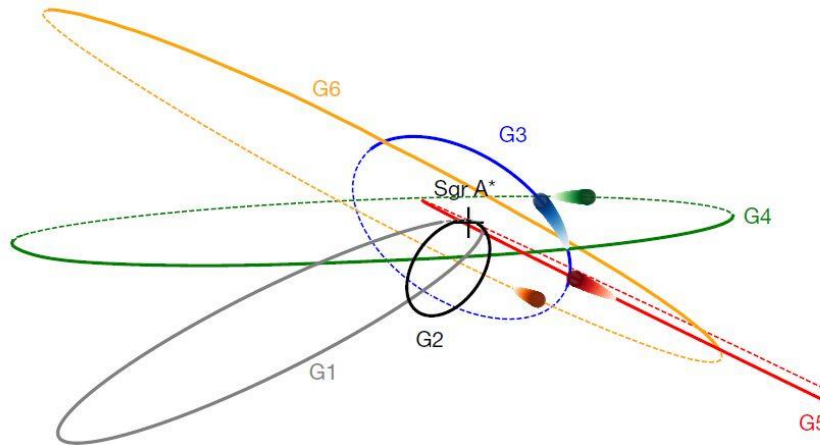
**Figure 4.** (Main figure) *XMM-Newton* (red) and *Chandra* (blue) light curves of the 2–10 keV flux emitted by Sgr A\*. Gaps between observations are removed. Dotted black vertical lines separate the different years or periods. The longest total exposure was obtained in 2012. The dashed violet vertical line indicates the start of the outburst of the magnetar SGR J1745-2900 on 2013 April 25 (§ 2.1). The pink box indicates the approximate time of the peri-center passage of G2 (Gillessen et al. 2013; Witzel et al. 2014). The dashed green horizontal lines roughly indicate the demarcation between weak, moderate, bright and very bright flares. The different flare types are defined here on the basis of their fluence and not by their peak count rates. The thresholds between weak and moderate and between moderate and bright flares indicate the average count rate for flare lengths of 1 ks. Longer flares lasting 1.7 ks are considered for displaying the threshold between the bright and very bright flares. The brightest flare has been detected on 2013 September 14 (Haggard et al. 2015). We note that, before 2013, weak, moderate and bright flares are randomly distributed within the 15 years of observations. This Sgr A\* light curve suggests a lack of moderate flares during 2013 and 2014, while we observe a series of 5 bright flares clustering at the end of 2014, several months after the peri-center passage of the bulk of G2’s material. (Upper panel) Zoom on the 2013–2014 period that shows that no moderate flare was observed, while 5 bright flares were observed right at the end of the *XMM-Newton* and *Chandra* monitoring campaigns. An additional bright flare (not shown here) was detected by *Swift* on October 10, 2014, right in the middle of the *XMM-Newton* monitoring campaign. These observations suggest an increased flaring rate of Sgr A\* during fall 2014.



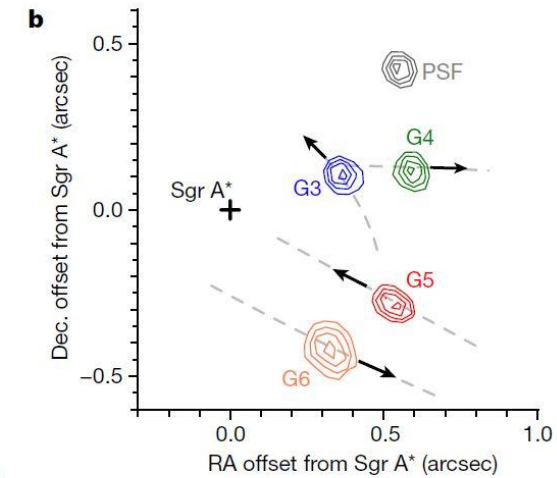
## Características de los objetos G:

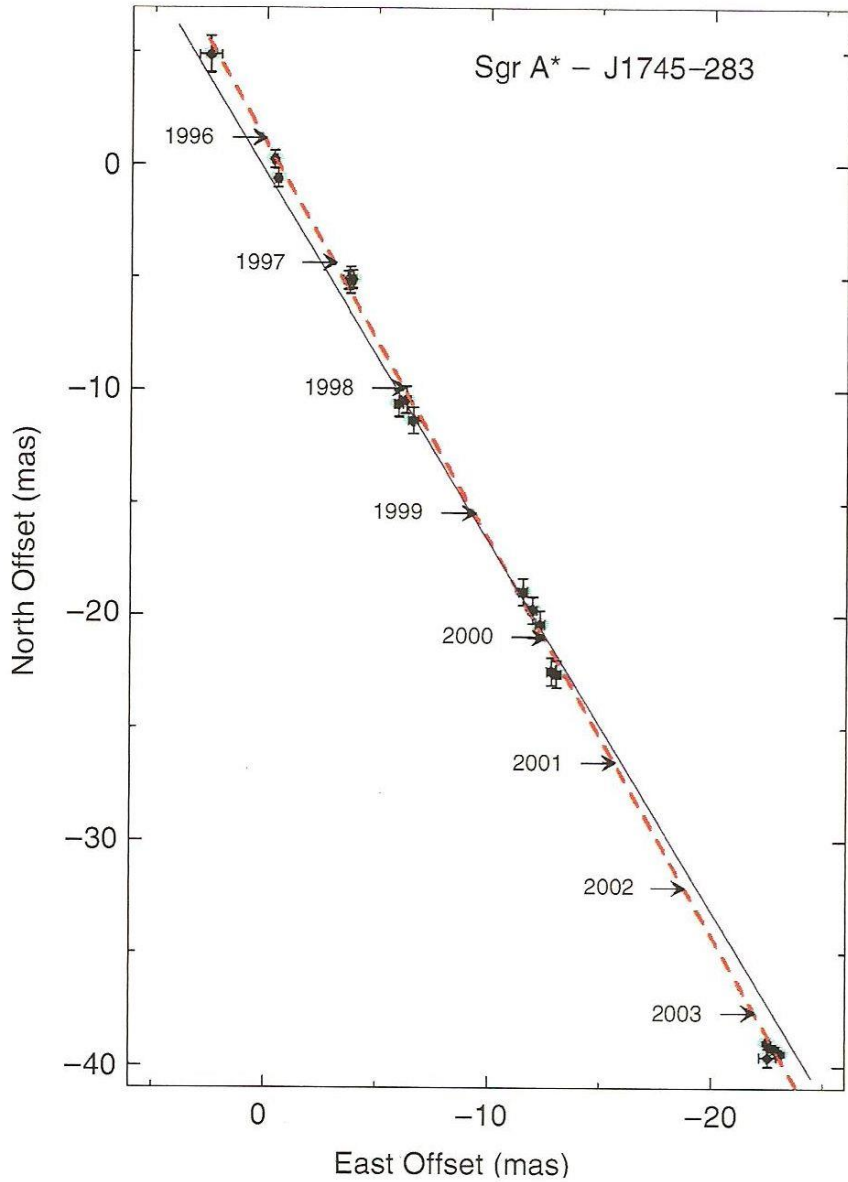
- 1) presencia de una fuente de **emisión Bry**
- 2) emisión espacialmente ( $\leq 0.05''$ ) **compacta**
- 3) emisión relativamente débil en la banda K
- 4) grandes **desplazamientos** en movimiento propio y velocidad radial
- 5) generalmente muy rojos (**pollo**):  $K'-L' > 5.2$
- 6) **menos masivos** que las **estrellas S** ( $> 1.5 M_{\odot}$ )

**Hipótesis:**  
**núcleo estelar**  
**poco masivo o**  
**sistema binario**  
**(edad de 4-6 Myr),**  
**envuelto por una**  
**nube extendida de**  
**gas ionizado y**  
**pollo.**



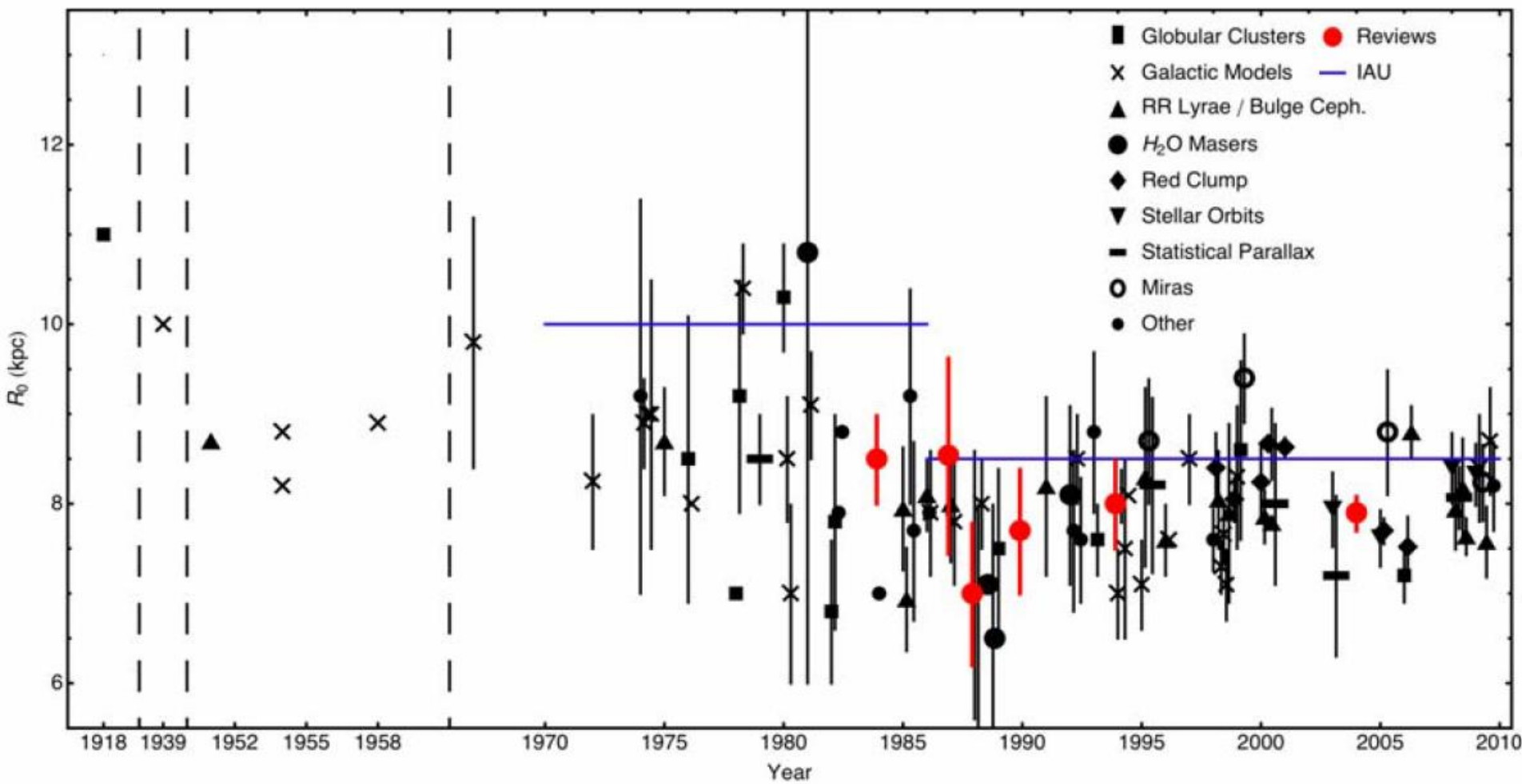
A. Ciurlo et al. 2020,  
Nature 577, 337-355





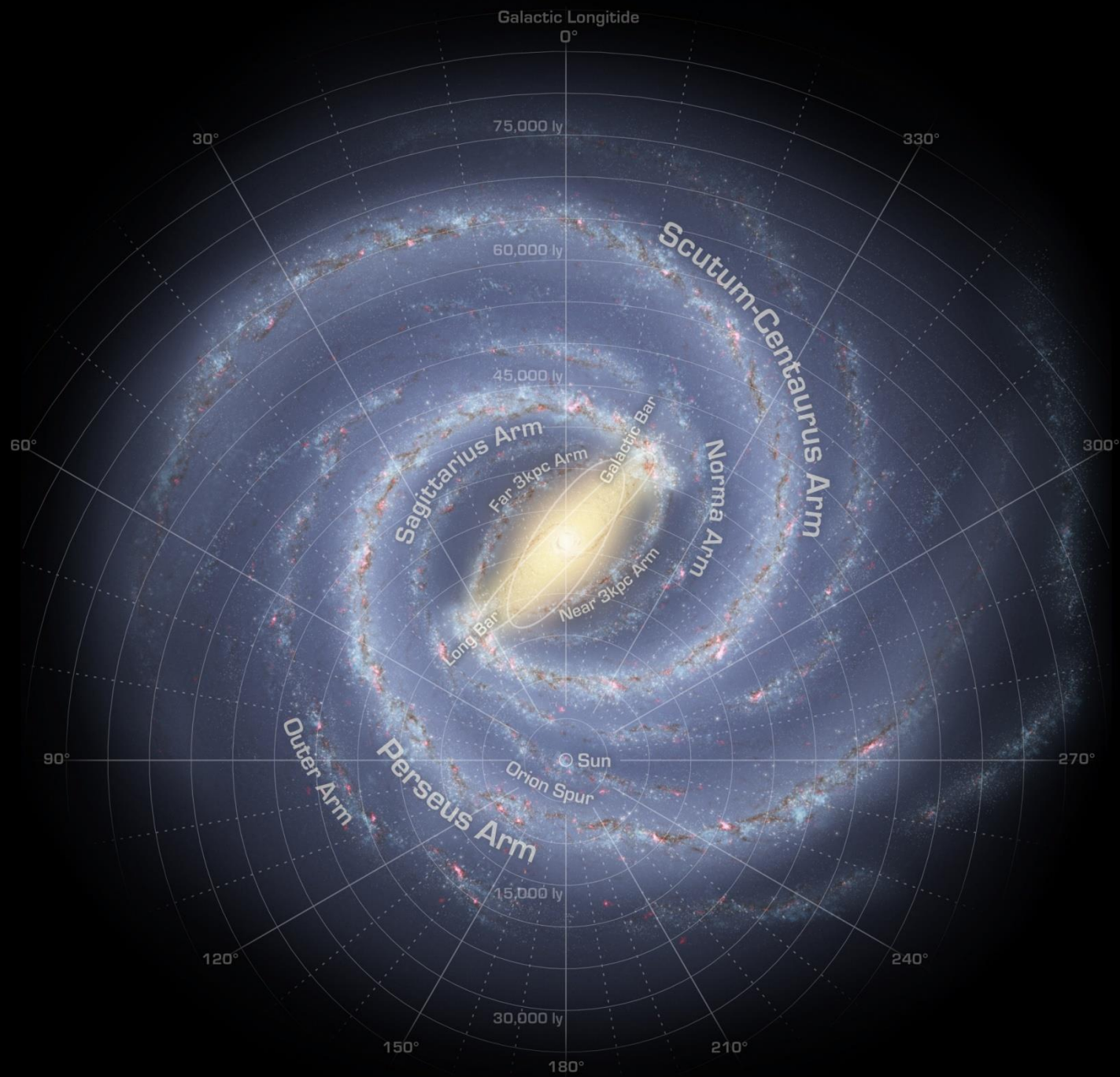
movimiento propio del Centro Galáctico  
 VLBI, respecto a 2 fuentes radio  
 extragalácticas, 8 años  
 $v_z = 0.2 \text{ mas/a}, v_\theta = 6.4 \text{ mas/a}$   
 $(241 \pm 15 \text{ km/s, para } R_0 = 8 \text{ kpc})$   
 $\Rightarrow$  movimiento orbital del Sol

**Fig. 2.39.** The position of Sgr A\* at different epochs, relative to the position in 1996. To a very good approximation the motion is linear, as indicated by the dashed best-fit straight line. In comparison, the solid line shows the orientation of the Galactic plane



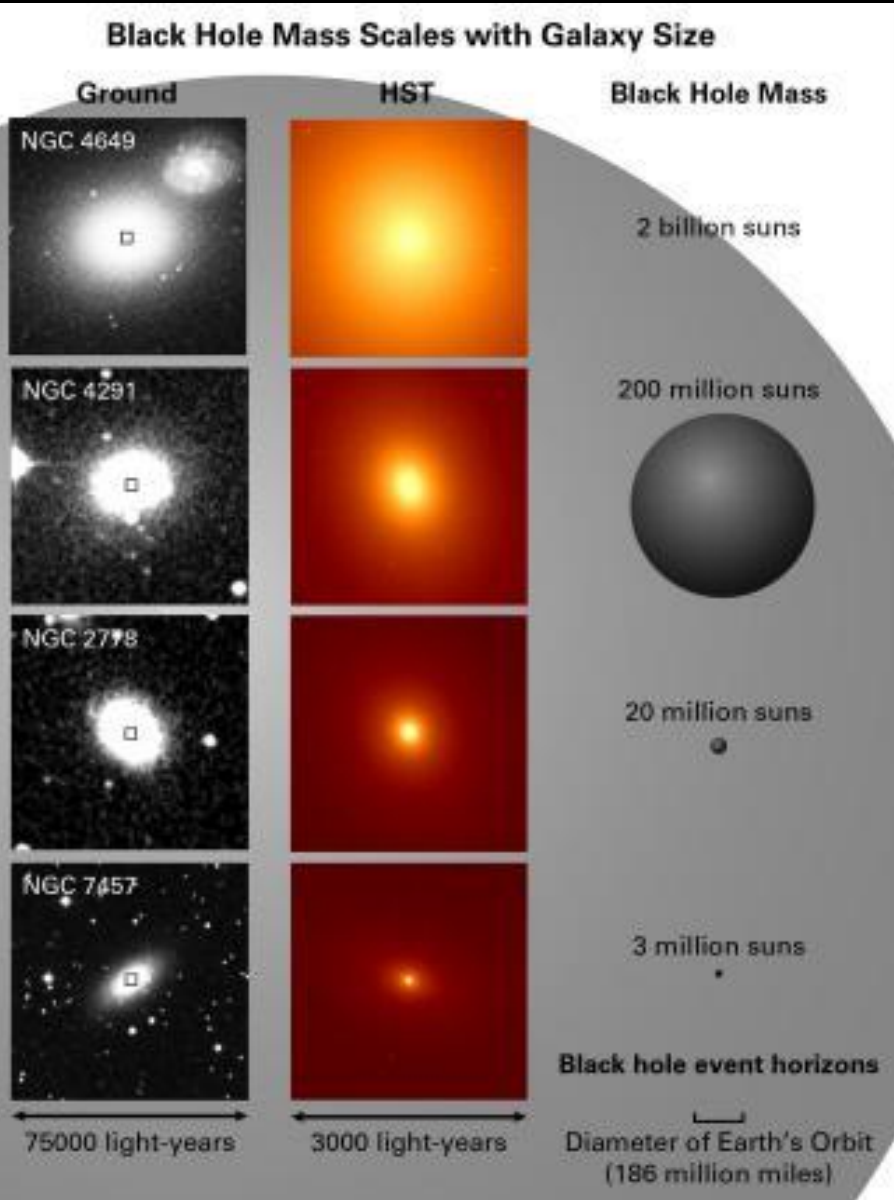
## **Tarea 5:**

Lectura: secciones 9.4 y 9.5 de Binney & Merrifield



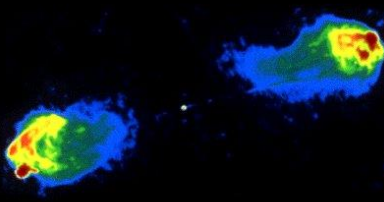
# ¿ Y más allá ?

NGC 7052





Cyg A



Cen A



For A

